Construction of Composite Membranes for Desalination and Adsorption of Heavy Metals

By
Aiza Zafar
Registration No. 02312113002

DEPARTMENT OF ENVIRONMENTAL SCIENCES
FACULTY OF BIOLOGICAL SCIENCES
QUAID-I-AZAM UNIVERSITY
ISLAMABAD, PAKISTAN
2021-2023

Construction of Composite Membranes for Desalination and Adsorption of Heavy Metals

A dissertation submitted in partial fulfilment of the requirement for the degree of
Master of Philosophy
in
Environmental Sciences

BY

Aiza Zafar

Registration No. 02312113002

DEPARTMENT OF ENVIRONMENTAL SCIENCE

FACULTY OF BIOLOGICAL SCIENCES

QUAID-I-AZAM UNIVERSITY

ISLAMABAD, PAKISTAN

2021-2023

PLAGIARISM UNDERTAKING

I, **Aiza Zafar**, here by state that my MPhil report thesis" **Construction of composite membranes for desalination and adsorption of heavy metals"** is solely my research work with no significant contribution from any other person. Small contribution/help whatever taken has been duly acknowledged and complete report has been written by me.

I understand zero tolerance policy of the HEC and Quaid-I-Azam University, Islamabad, towards plagiarism. Therefore, I as an author of the above titled report declare that no portion of my report has been plagiarized and a reference is properly referred or cited for any material used.

I undertake that if I am found guilty of any form of plagiarism in the above tilted report even after the award of MPhil degree, the university reserves the right to withdraw/revoke my MPhil degree and that HEC and the university has the right to publish my name on the HEC/University website on which the names of students are placed who submitted plagiarism.

Aiza Zafar

AUTHOR'S DECALARATION

I **"Aiza Zafar (Registration No. 02312113002)"** hereby state that my MPhil thesis titled as **"Construction of composite membranes for desalination and adsorption of heavy metals"** was carried out by me in the Renewable Advancement Laboratory, Department of Environmental Sciences, Quaid-I-Azam University, Islamabad. The results, findings, conclusions and investigations of this research has not been previously presented and not been published as a research work in any other university.

Aiza Zafar

Reg No. 02312113002

CERTIFICATE OF APPROVAL

It is to certify that the research work presented in this MPhil thesis, entitled **"Construction of composite membranes for desalination and adsorption of heavy metals."** was conducted by Aiza Zafar **(Reg. No. 02312113002)** under the supervision of **Dr. Abdullah Khan.** No part of this thesis has been submitted else for any other degree. This report is submitted to the **Department of Environmental Sciences,** in the partial fulfillment of the requirements for the degree of **Masters of Philosophy** in the field of Environmental Science, Quaid-i-Azam University, Islamabad, Pakistan.

Aiza Zafar _____

Supervisor:

Dr. Muhammad Abdullah Khan _____

Associate Professor
Department of Environmental Sciences
Quaid-i-Azam University, Islamabad.

Chairperson:

Dr. Abida Farooqi _____

Associate Professor
Department of Environmental Sciences
Quaid-i-Azam University, Islamabad

Date: _____

ACKNOWLEDGMENT

First of all, I am grateful to Allah Almighty who blessed me with this precious life and all the abilities I got. I am very thankful to HIM for the countless blessings He has bestowed upon me particularly an opportunity to get education in one of the prestigious institute which many people dream of.

I am extremely grateful to **Dr. Abdullah Khan** who has guided me throughout this degree program and supported me through all ups and downs.

After that, I want to thank my entire family especially my mother, husband and siblings for helping me out in all possible ways. I dedicate this research to my mother.

I want to extend my special gratitude towards senior fellows for guiding us at every step.

I want to especially thank my friends and colleagues **Fariah Salam**, Nimra Zafar Cheema, Tooba Hassan, Rimsha Khan, Mahnoor Adnan, Amna Shafique and Shehla Asghar.

I especially want to thank Mr. Ayub Khasana for his providing me with every equipment and machinery.

In the end, I am grateful to Allah Almighty for blessing and rewarding me with all these precious people, without them, I am nothing.

Aiza Zafar

LIST OF ACRONYMS

WHO	World Health Organization
UNDP	United Nations Development Programme
RO	Reverse Osmosis
FO	Forward Osmosis
SWRO	Seawater Reverse Osmosis
MD	Membrane Distillation
ED	Electrodialysis
MSF	Multi-stage flash Distillation
MED	Multi-effect flash Distillation
TFC	Thin-film Composite
J_w	Water flux
VCD	Vapour Compression Distillation
q_e	Adsorption Capacity
R_s	Salt Rejection Rate
GO	Graphene Oxide
rGO	Reduced Graphene Oxide
LDH	Layered Double Hydroxide
XRD	X-ray Diffraction Spectroscopy
SEM	Scanning Electron Microscopy
FTIR	Fourier-transform Infrared Spectroscopy
AAS	Atomic Absorption Spectroscopy

TABLE OF CONTENTS

LIST OF TABLES

LIST OF FIGURES

HIGHLIGHTS

- Nanocomposite membranes of varying wt% (3%, 7% and 10%) are synthesized.
- The efficacy of membranes is checked for heavy metal adsorption, desalination and simultaneous activity of both.
- 10% rGO/NiMoV LDH membrane exhibits maximum efficiency with 100% Pb (II) removal and 99.9% desalination activity.
- The nanocomposite membrane showed maximum adsorption at pH = 8, catalyst dose = 10 mg and pollutant concentration = 40 ppm.
- The maximum water flux i.e. 49 LMH is observed in 7% rGO/NiMoV LDH.
- In simultaneous activity, the desalination and adsorption efficiency of the membrane decreased by 3%.

GRAPHICAL ABSTRACT

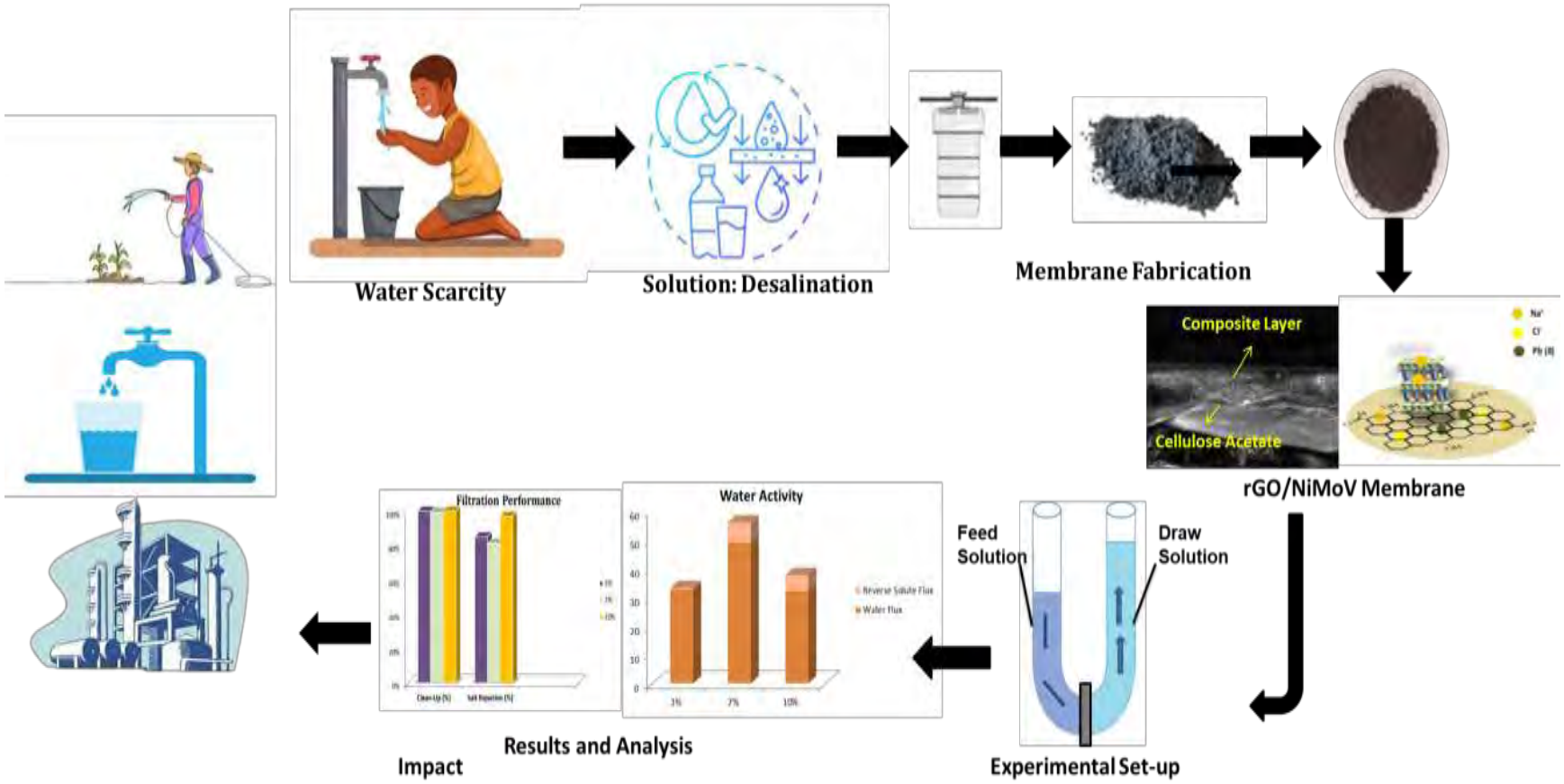

ABSTRACT

Freshwater scarcity and heavy metal toxicity is a pressing global issue which has provoked the scientific community to look for energy and cost-efficient seawater treatment techniques. In this research study, TFC membranes of rGO/NiMoV LDH are synthesized with varying wt% of rGO i.e., 3%, 7% and 10%. The physiochemical properties of fabricated membranes are analyzed with characterization techniques i.e., scanning electron microscopy (SEM), X-ray diffraction (XRD) and Fourier-transform infrared spectroscopy (FTIR). The TFC membranes were tested for desalination and adsorption of heavy metal through forward osmosis individually and simultaneously both. The results showed that by increasing the wt. % of rGO in TFC membranes, the desalination performance and adsorption efficiency increased. The highest desalination performance is shown by 10% rGO/NiMoV LDH with 100% Pb (II) adsorption. When analyzed for simultaneous operation, there was a slight decrease in desalination and adsorption both due to increased competing effect of Pb (II), Na^{+}, and Cl^{-} ions. Additionally, effect of pH, composite dose and pollutant concentration is also investigated for adsorption. This study serves as a milestone to achieve simultaneous desalination and heavy metal adsorption by forward osmosis which can be a basis for further research and development in seawater treatment.

1. INTRODUCTION

1.1. Background

To ensure a healthy and well-sustained environment, water is an important resource. Almost one-third of the Earth's surface is covered by water. Out of total water cover, approximately 97% is seawater and 2% is in the form of ice, held in glaciers. Water seems an abundant resource but freshwater resources are scarce and unavailable for human use. The past century has been marked by exponential industrial growth and population increases. Over the past decade, there has been an increasing awareness in society about the importance of freshwater resources, their vulnerability, and scarcity. Many countries are facing extreme scarcity of freshwater resources such as Lebanon, Pakistan, Afghanistan, Syria, and Turkey. Increasing population and expanding industrial and agricultural needs is putting stress on freshwater resources. The World Health Organization (WHO) has highlighted the scarcity of freshwater resources by addressing that one-quarter of the world's population is living in water-stressed countries as they lack the necessary resources to draw freshwater from streams, aquifers, and rivers [1].

Figure 1: Water scarcity map by WHO

Considering the availability of immense seawater resources of some water scarce countries, desalination is a viable and effective option for them. The desalination of seawater should be carried out in such a manner that it is appropriate for human consumption. Desalination is an effective technique to separate out salts from water and convert the seawater into pure water containing lesser salts concentration.

According to statistical data, almost 75 million people use water which has been purified by desalination of sea or brackish water.

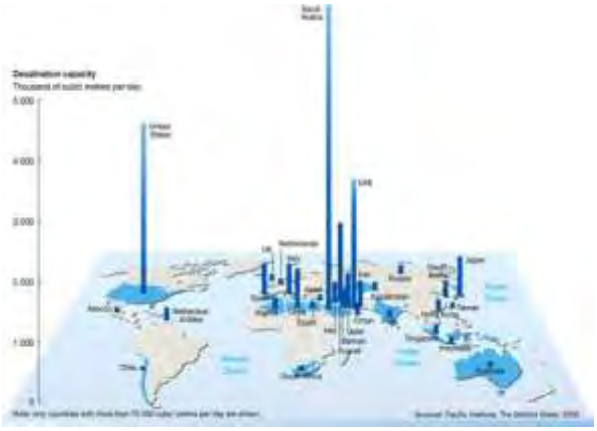

Figure 2: Map displaying desalination capacities of different countries

Source: Pacific Institute, The World Waters, 2009.

In 1951, Pakistan was a country with abundant water having freshwater availability of 5000 m^3 per capita while in 2015, it is facing extreme scarcity having declining per capita water availability i.e., 1100 m^3 per capita [2].

United Nations Development Program (UNDP) for Pakistan said that increasing water scarcity in Pakistan is due to substandard management of present water resources, climate change and rising population. Based on first two water scarcity causes, it is recommended to increase the supply of water by strengthened infrastructure i.e., desalination plants. The World Bank has also suggested increasing the capital investment in desalination infrastructure to cater water scarcity. The total desalination capacity of Pakistan in 2015 was 188,168 m^3/day [1,2].

The conventional desalination techniques i.e., Multi-stage flash distillation and reverse osmosis (RO) need immense energy that is cost-inefficient and environmentally unsustainable. To cater the increasing water needs economically, innovative and cost-effective desalination methods are needed. Thus, it has become a prime focus of the scientific society to find effective desalination methods. This research work is undertaken to discover the desalination potential of forward osmosis (FO) as a cost-effective and efficient water treatment technique.

The results of this research can be executed by water authorities within Pakistan to cater the water scarcity problem with forward osmosis (FO) on a national-level with low energy costs and investment. Forward osmosis for desalination is an effective technique to reduce the water production costs and can be implemented as a finest and low cost water treatment method [3].

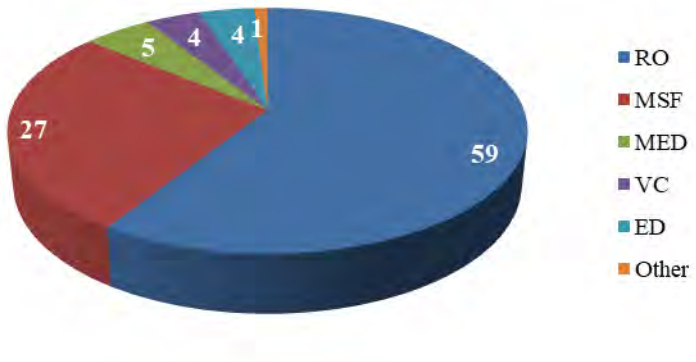

Figure 3: Water production by different distillation processes

1.2. Osmotic Membranes

Desalination carried out by reverse osmosis is commonly dependent on membrane (used in the process) characteristics and properties. The most important synthetic materials for osmotic membranes are polyamides and cellulose acetate that reject the salts and ensure the passage of water at an appropriate speed. A suitable membrane should has high water flux, salt rejection, resistant to biological attacks, antifoulant, cost-effectiev, chemically stable, resistant to high pressures and temperatures [4].

Thin-film composite membranes have multiple polymer layers and asymmetric membranes having one polymer layer. Thin-film composite membranes for reverse osmosis consist of a thin polymer layer supported on multiple porous layers. The surface layer is always different from the support polymer layer. The water flux and separation selectivity is determined by the membrane's surface layer whereas; the support for the surface layer is given by the porous layer. It has no impact on transport and separation membrane properties [5].

1.3. Energy Efficient Desalination Techniques – Forward Osmosis

Forward osmosis (FO) is gaining attention as a cost-effective and energy-efficient desalination method amid the growing demand for fresh water. Numerous studies explore its applications in water purification, wastewater treatment, and desalination. Compared to reverse osmosis (RO), FO is more energy-efficient. Research emphasizes enhancing FO by using high osmotic pressure draw solutions, efficient water membranes, and energy-efficient processes for water recovery. FO's potential spans across various fields like water desalination, energy production, and wastewater treatment[6]. Enhancing FO primarily focuses on developing flat-sheet and hollow fiber membranes with improved water permeability, decreased internal concentration polarization (CP), high salt rejection, and enhanced chemical and mechanical stability[7].

1.4. Forward Osmosis Theory

1.4.1. Calculation of Osmotic Pressure

The osmotic pressure of dilute solutions is measured by using Van't Hoff equation:

$$\boldsymbol{\pi = MR} \ldots\ldots\ldots\ldots\ldots\ldots \textbf{Eq. 1. 1}$$

where π is the osmotic pressure in bars, M is the solute molar concentration in moles/liter, R is the universal gas constant (0.08314 L bar mol^{-1} K^{-1}), and T is the temperature in Kelvins. However, for concentrated salt solutions such as the draw solution in FO, the non-ideal solution behavior must be accounted and the osmotic pressure is calculated as follows [8]:

$$\boldsymbol{\pi = \emptyset MRT} \ldots\ldots\ldots\ldots\ldots\ldots \textbf{Eq.1.2}$$

Where M represents solute molar concentration in moles/liter, π represents osmotic pressure in bars; R is universal gas constant with value of 0.08314 L bar mol^{-1} $K^{-1}$and T is temperature in kelvins. In case of concentrated solutions in FO, the osmotic pressure is calculated as:

$$\boldsymbol{\pi = \phi MRT} \ldots\ldots\ldots\ldots\ldots\ldots \textbf{Eq. 1. 3}$$

In the above equation, ϕ is osmotic pressure coefficient. Particularly, the ideal solute deviation is handled by Virial equation.

1.4.2. Water Flux Calculation

Volume change in the feed and draw solution can be used to calculate the water flux during forward osmosis (FO) experiment. When FO process goes forward, the volume of the feed solution decreases as the water flows from feed to draw solution. The water flux can be measured by:

$$J_w = \frac{\Delta v}{s\Delta t} \text{.....Eq. 1.4}$$

In the above equation, ΔV is the volume change of draw or feed solution, S represents the membrane area involved in water flux and Δt is the time in which the volume change between feed and draw solution occurs.

1.4.3. Water flux Model

Following the traditional solution-diffusion theory, water flux (J_w) for forward osmosis (FO) is same as other membrane filtration processes:

$$J_w = A(\Delta P - \Delta \pi) \text{ ... ... Eq. 1. 5}$$

In the above equation, difference of hydraulic pressure across membranes is denoted by ΔP and osmotic pressure by Δπ.

The main working force in FO is differential osmotic pressure, therefore the equation for theoretically measuring the water flux in FO is:

$$J_w = A\left(\pi_{D,b} - \pi_{f,b}\right) \text{ ... ... Eq. 1. 6}$$

where $\pi_{D,b}$ is the bulk osmotic pressure of the draw solution , $\pi_{F,b}$ is the bulk osmotic pressure of the feed solution and A is the membrane water permeability coefficient. According to the equation, the FO membrane is impermeable to draw solution.

$$J_w = \frac{1}{K}\ln\left[\frac{A\pi_{Draw}+B}{A\pi_{Feed}+B+J_w}\right] \text{.....Eq. 1.7}$$

In the above equation K denotes the resistance of membrane porous support layer towards solute diffusion. K is defined by the following equation, if all polarization effects are neglected:

$$\boldsymbol{B = \frac{(1 - R)A(\Delta P - \Delta \pi)}{R}} \ldots\ldots\ldots\ldots\ldots\ldots \textbf{Eq. 1.8}$$

In the above equation, t is the membrane thickness, τ is tortuosity, ε is porosity and Ds solute diffusion coefficient.

1.4.4. External Concentration Polarization (ECP)

Membrane-related factors, like internal and external polarization, impact water flow in FO and other osmotically-driven processes. In forward osmosis, concentration polarization happens as feed water moves to permeate, causing salt deposition and scaling on the membrane. This occurs similarly in both osmotic and pressure-driven membranes. External concentration polarization notably increases flow velocity and turbulence on the membrane, but in FO, its impact is minimal due to low hydraulic pressure.[5].

1.4.5. Internal Concentration Polarization (ICP)

Forward osmosis membranes are generally uneven in which active layer is deposited on porous support. Polarized layer is produced on the uneven dense surface of membrane when porous support is in contact with feed solution. As a result the osmotic pressure across the membrane decreases. This phenomena is known as internal concentration polarization (ICP). ICP is same as ECP but it occurs on membrane porous support layer and cannot be reduced by altering the turbulence and flow rate of the membrane surface.

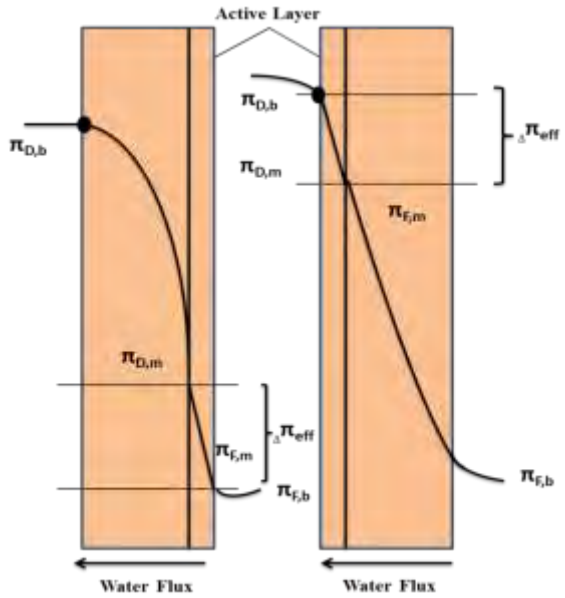

Figure 4: Diagram for internal concentration polarization

1.4.5.1. Modeling Internal Concentration Polarization (ICP)

Following analytical equation measures the cumulative impact of both dilutive ECP and concentrative ICP [8]:

$$J_w = A\left[\pi_{Draw}\exp\left[-\frac{J_w}{K} - \pi_{feed}expJ_wK\right]\right] \ldots\ldots\ldots\ldots\ldots\ldots \textbf{Eq. 1.9}$$

1.5. Previous Forward Osmosis Desalination Efforts – Literature Review

1.5.1. Forward Osmosis Membranes

Different membranes have been synthesized and analyzed for forward osmosis. Selectively permeable and dense membranes are suitable forward osmosis applications. Moreover, membranes showing reduced ICP and lower porosity is preferable for support layer. Some suitable characteristics for a forward osmosis (FO) membrane are high water permeability, low reverse solute flux, chemical stability, mechanical strength and high salt rejection rate [9].

Rubber, porcelain, nitrocellulose, fish skin and animals' bladders were used to make first forward osmosis membranes [10,11]. B-9 RO flat sheets and B-10 hollow fiber Permasep RO membranes are also employed for FO applications [12]. In recent research

studies, cellulose ester polymer membranes for desalination by forward osmosis. For forward osmosis desalination polybenzimidazole (PBI) nanofiltration membranes are employed for the first time which has shown good chemical stability and mechanical strength [4,13].

1.5.2. Forward Osmosis Draw Solutions

The high osmotic pressure of the draw solution is the source of driving force for water in FO process. The main force for carrying FO processes is provided by osmotic pressure of draw solution. The draw solution is also called osmotic media, engine, agent or driving force [14]. The main property for a draw solution in forward osmosis processes is high osmotic pressure compared to feed solution. The FO processes are viable when osmotic pressure is higher at draw solution side. Draw solution employed in FO should be recyclable, energy-efficient, non-toxic, chemically stable, have high solubility and osmotic pressure [15,16].

1.6. Limitations of Forward Osmosis in Desalination

Through research studies it has been shown that there are two principle shortcomings which are need of highly efficient membranes and recoverable draw solution. Due to various factors such as polarization effects, water flux in FO membranes decreases. Therefore, scientific community is working for synthesizing suitable FO membranes showing maximum salt rejection, lower concentration polarization, chemical stability and good mechanical strength. Additionally, previously employed FO processes need immense energy for water recovery from draw solution. Heating or pressure is needed for recovery of product water from draw solutes. Therefore, perpetual research work is being done for low energy recovery methods for draw solution.

1.7. Adsorption of Lead Pb (II) by Forward Osmosis

1.7.1. Background

Water is extremely essential for life sustenance. There are three main sources of obtaining water i.e., surface water, groundwater and rainwater. Due to the increasing population, the demand for water consumption is increasing day by day. Water for

drinking and consumption purposes should be free of any hazardous heavy metal. But water sources in Pakistan are contaminated with many heavy metals like chromium, lead, mercury, cadmium etc. which impact human and environmental health badly. Elements having specific gravity five times greater than water and atomic weight between 63 and 200 are known as heavy metals (HMs). HMs are non-biodegradable therefore in living organisms these cause disorders and diseases. Three big heavy metals which are most important due to their intense bad impact are Cadmium (Cd), Lead (Pb) and Mercury (Hg). Lead and cadmium are potential neurotoxins which disrupt human neurological functions. Lead is a poisonous heavy metal which disrupts enzymatic functions by making complexes with the oxo-groups impacting the entire process of porphyrin metabolism and hemoglobin synthesis. Besides this, lead damages the nervous, renal, liver, brain and cardiac systems. Prolonged exposure to lead can cause infertility, still-births, abortions and neonatal mortalities [17].

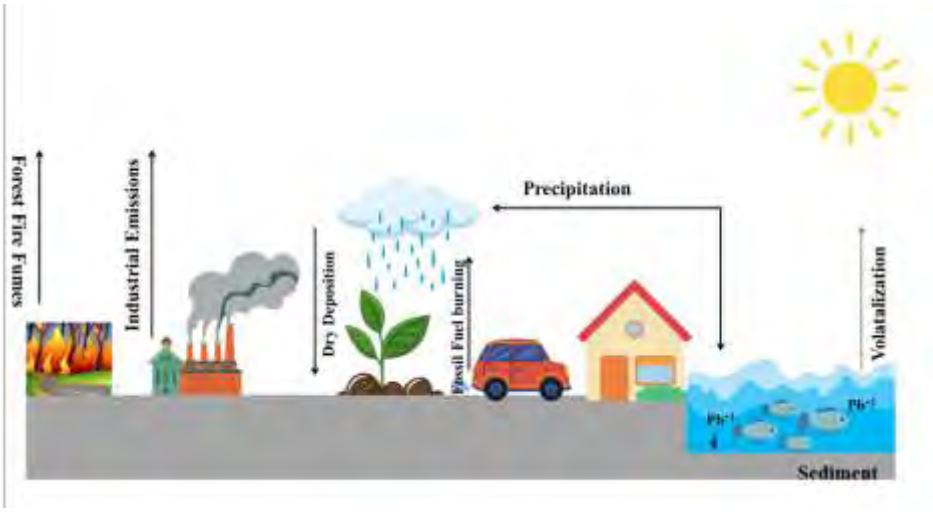

Figure 5: Sources and pathway of lead in atmosphere

WHO has devised a maximum permissible limit (MPL) of 0.01 mg/l of Pb (II) in drinking water whereas for wastewater the value is 0.05mg/l. As lead is extremely harmful for human and environmental health therefore its proper treatment and removal from the ecosystem is necessary. There are different techniques for heavy metal removal from water i.e., coagulation, precipitation, ion exchange, electrolysis, reverse osmosis, solvent extraction and adsorption. Most of the removal processes are expensive, infeasible and non-friendly to the ecosystem due to disposal and secondary pollutants and residual sludge. The most viable, applicable and feasible technique for heavy metal removal is adsorption as it is cost-effective and its design is simple [18].

1.7.2. Status of Lead Toxicity in Pakistan

In developing countries, water contamination is a main cause of health ailments. Drinking water contaminated with lead can impart harmful impacts on different body systems such as renal, nervous, reproductive and hematopoietic systems particularly in children. The main routes of lead exposure are inhalation, ingestion and absorption. Almost 35%-50% of lead present in drinking water is absorbed in adults and 60% lead is absorbed in children. Pakistan is a developing country where there is less number of studies conducted on impacts and routes of lead toxicity [17]. In Karachi, which is a metropolitan city, excess amounts of lead are detected in drinking water. A study has shown that there is a deep association between hypertension and increased lead levels in blood in Pakistan's population. It is reported that half of the children in Pakistan have higher lead levels than normal. There are different sources of lead toxicity in Pakistan such as cosmetics, drugs, paint, and cloth manufacturing and battery industries. In the atmosphere, lead has been released by petroleum-fuel burning. Rapid urbanization and industrialization has increased water pollution issues in megacities of Pakistan such as Karachi. Improper water management has provoked chemical and biological contamination of surface and groundwater. This is contaminating the major water body i.e., Arabian Sea which is a habitat to a variety of ecosystems. Another source of lead contamination of Arabian Sea is maritime vehicles. The health impacts of lead toxicity are apparent in Pakistan's population. The chronic symptoms are insomnia, headaches, tiredness and gastrointestinal problems[19]. Therefore, there is a need to handle lead toxicity in water resources to cater to the deleterious health impacts of lead on Pakistan's population.

1.7.3. Conventional Methods for Heavy Metal Removal

Following figure explains the working principles of conventional heavy metal removal techniques which are chemical precipitation, flocculation and coagulation, ion exchange and adsorption.

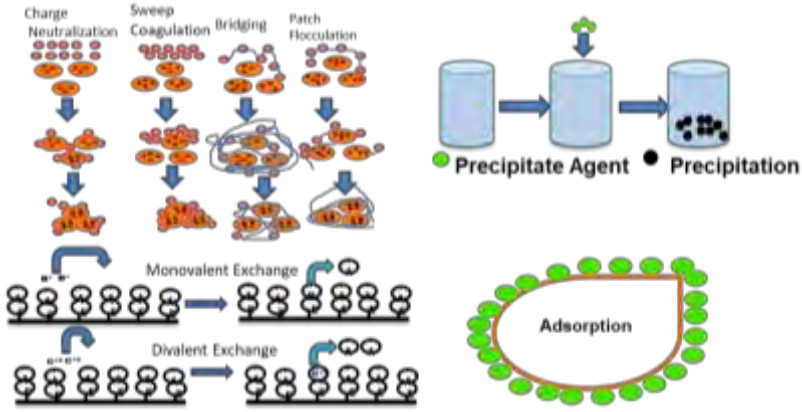

Figure 6: Conventional methods for heavy metal removal

1.7.4. Membrane filtration

There are a number of membrane filtration methods based on membrane types. As compared to conventional heavy metal removal methods, membrane filtration has many advantages i.e., high surface area, high separation, involve no phase transition, energy-efficient and environmental friendly. There are different types of membrane filtration techniques such as ultrafiltration, reverse osmosis and nanofiltration. Following figure explains the difference between membrane filtration techniques.

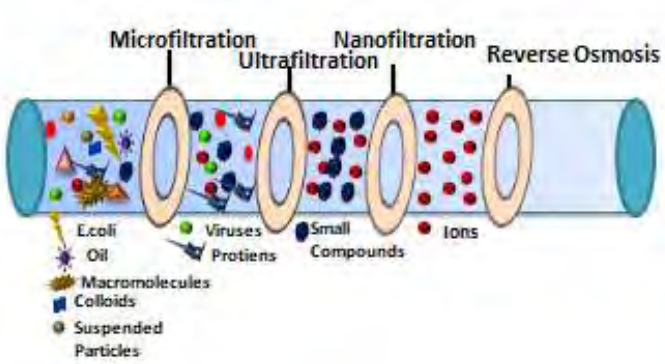

Figure 7: Difference between membrane filtration techniques

1.7.5. Adsorption

Adsorption is an important process for wastewater treatment and environmental remediation. It has a significant role in contaminant removal from wastewater. In the process of adsorption, the ions or molecules are adhered to the material (adsorbent) surface. The active sites present on the surface of adsorbent can attract and hold the contaminant which can be resultantly removed from the solution. For developing an

efficient water treatment technique, it is essential to understand the principles and mechanism of adsorption to optimize adsorbent composition and material properties [20].

1.7.5.1. Mechanism of Adsorption

Adsorption is basically a surface phenomenon in which the ions, molecules or particles from liquid or gas medium adhere or adsorb on the surface of adsorbent (solid phase). The attractive forces between adsorbent and adsorbate work to accumulate the particles on the surface of adsorbent.

There are several steps involved in adsorption mechanism which are adsorbate deposition on adsorbent surface, interaction of adsorbent-adsorbate, adsorption at active sites, adsorption equilibrium, monolayer and multilayer adsorption, desorption and regeneration [21].

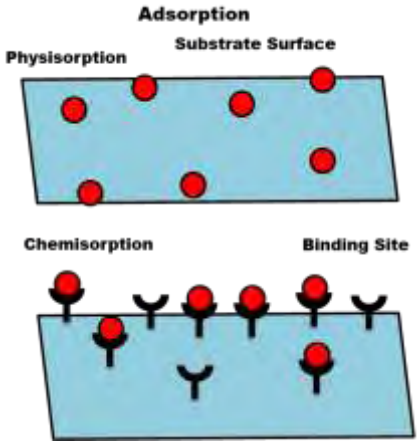

Figure 8: Mechanism of adsorption

1.7.5.2. Factors Affecting Adsorption

Lately, there has been a significant rise in the use of nanomaterials or modified nanomaterials to eliminate harmful heavy metals from wastewater. This increase can be attributed to the unique characteristics of these materials, such as their large surface area and enhanced ability to bind heavy metals attributed to specific functional groups. The nanomaterial-based adsorbents currently employed in wastewater treatment have undergone substantial advancements and can be classified based on the material used or modified to create the nanoadsorbent. Several factors,

including pH, temperature, contact time, and concentration, have an impact on the adsorption process. Adsorption process is influenced by pH, based on the presence of functional groups on the surface of the adsorbent material [22]. The efficiency of removal is seen to increase steadily in the beginning with an increase in contact time, and then it slows down, after the active sites get occupied. When more absorbent is added, there are more places for adsorption to happen, which improves how well adsorption works. Increasing the adsorbent dose is beneficial only until it increases the number of active sites, but after that, efficiency decreases because of agglomeration. When the temperature rises initially, it causes a decrease in the thickness of the solution, resulting in improved spreading ability and, consequently, enhanced ability to attract particles. The ability to adsorb depends on the strength of the aqueous solution, which is influenced by additional ions commonly found in wastewater samples [21].

1.7.5.3. Adsorption Isotherms and Kinetics

To grasp how nanoparticles interact with heavy metals, scientists have put forth different theories on the speed and extent of adsorption. These theories aim to establish a state of balance in the adsorption process. Various factors, including the initial concentration of ions, temperature, duration of contact, amount of adsorbent used, and pH level, can influence the adsorption of heavy metals onto the surface of nanoparticles. In this study, we have dedicated separate sections to discuss both the adsorption kinetics and isotherms [23].

1.7.5.3.1 Adsorption Isotherms

Adsorption isotherms are crucial for figuring out how much adsorbent materials can hold. They show the balance between the adsorbent and what is being adsorbed at a specific temperature. Different models, like Langmuir, Temkin, Freundlich, Dubinin-Radushkevich, and Sips, have been used to describe adsorption isotherms.

1.7.5.3.1.1. Langmuir Model

This model describes the monolayer adsorption between adsorbent and solute. When the adsorbates fill the adsorption sites, there are no more adsorption sites, and the strength of their connection stays the same on all the available spots. Each spot can

only hold one adsorbate. The Langmuir model uses the following linear equation to measure this adsorption.

$$\frac{c_e}{q_e} = \frac{1}{Q^{ob}} + \frac{C_o}{Q_o} \ldots\ldots\ldots\ldots Eq.\ 1.10$$

In above equation, equilibrium concentration is denoted by C_e, concentration of adsorbed metal by q_e, Langmuir constant by b and monolayer adsorption capacity by Q_o.

1.7.5.3.1.2. Temkin Isotherm

Temkin isotherms show how the consistent distribution of bonding energies corresponds to the highest level of energy utilized during the process of adsorption. It explains how the temperature of adsorption molecules decreases in a straight line as the interaction between adsorbate and adsorbent molecules intensify. The equation that represents the Temkin isotherm is as follows:

$$q_e = BlnA_t + BlnC_e \ldots\ldots\ldots\ldots\ldots\text{Eq. 1.11}$$

In above equation, equilibrium concentration is denoted by C_e, concentration of adsorbed metal by q_e, Temkin constant by A_t and heat constant by B.

1.7.5.3.1.3. Freundlich Model

It is an empirical equation that explains how adsorption behaves when the surface of the material is not smooth and multiple layers are formed. This mathematical model aligns well with the idea that adsorption sites are distributed exponentially. The equation represents the relationship between non-uniform adsorption and the roughness of the adsorbent surface.

$$logq_e = logK_f + \frac{1}{n} logC_e \ldots\ldots\ldots\ldots\ldots\text{Eq.1.12}$$

In above equation, equilibrium adsorbate concentration is denoted by C_e, concentration of adsorbed metal (adsorption capacity) by q_e, Freundlich constants by n and K_f.

1.7.5.3.1.4. Dubinin–Radushkevich Isotherm Model

This model is exceptionally well-suited for analyzing how heavy metals bind to nanoparticles, particularly carbon-based nanomaterials. It provides more

comprehensive understanding and outcomes compared to the Freundlich and Langmuir models when it comes to studying the attachment of molecules onto carbon nanoparticles and nanotubes. To summarize, this model can be represented as:

$$q_e = (q_s)exp + (-K_{ad}\varepsilon^2) \text{.....Eq. 1.13}$$

In above equation, concentration of adsorbed metal (adsorption capacity) is denoted by q_e, saturation capacity by q_s and K_{ad} is Radushkevich constant.

1.7.5.3.1.5. Sips Isotherm

The Sips isotherm is a unique model that combines elements of the Freundlich and Langmuir isotherms. It is employed to study the process of heterogeneous adsorption, overcoming the limitations of the Freundlich model. The equation representing the Sips isotherm is given by:

$$q_e = \frac{q_m + (K_s C_e)^{ns}}{1 + (K_s C_e)^{ns}} \text{.....Eq.1.14}$$

In above equation, adsorbate equilibrium concentration is denoted by C_e, concentration of adsorbed metal (adsorption capacity) by q_e, Sips adsorption by q_m, nS is factor of Freundlich heterogeneity, K_s is Langmuir equilibrium.

1.7.5.3.2. Adsorption Kinetics

The speed at which a reaction occurs is determined by adsorption kinetics. This involves understanding how the concentration of the reactant changes over time when it comes into contact with other substances. Different models have been suggested to explain this process, such as the pseudo-first-order kinetics, second-order kinetics, double exponential model, and intra-particle diffusion model.

1.7.5.3.2.1. Pseudo-first-order Kinetics

The concept of pseudo-first-order kinetics is employed to calculate the adsorption capability in both liquid and solid environments. This approach relies on the following linear equation that describes the behaviour of first order kinetics.

$$\log(q_e - q_t) = logq_e - \frac{K1}{2.303}t \text{ ..... Eq. 1.5}$$

Where, K_1, q_e and q_t are pseudo-first order kinetic constant, slow step adsorption rate parameters, adsorption concentration at equilibrium and time t (min).

1.7.5.3.2.2. Second-order kinetics

It is exclusively utilized within solid-phase systems and serves to determine the capacity for adsorption. The mathematical equation employed to represent the second-order kinetics is as follows:

$$\frac{t}{q_1} = \frac{1}{K_2 q_e^2} + \frac{1}{q_e} t \text{.....Eq. 1.16}$$

Where, K_2, q_e and q_t are pseudo-second order kinetic constant, slow step adsorption rate parameters, adsorption concentration at equilibrium and time t (min).

1.7.5.3.2.3. Double Exponential Model

There are also two-step processes documented for the absorption of toxic metal particles. Initially, the ions are absorbed through both internal and external diffusion. The mathematical representation of this model can be expressed as:

$$q_t = q_e - D_1 m_{ads} e^{-KO_2 t} \text{.....Eq. 1.17}$$

Where, D_1, D_2, q_e and q_t are rapid step adsorption rate parameters, slow step adsorption rate parameters, adsorption concentration at equilibrium and time t (min).

1.7.5.3.2.4. Intra-Particle Diffusion Model

This model is built upon the Morris and Weber theory, which explains the complex process of adsorption in multiple steps. It involves the movement of the substance being adsorbed to the molecules of the materials being adsorbed onto by transferring molecules into the solid pores of the material. The values of C and K id can be determined by calculating the intercept and slope of the straight-line graph showing the relationship between $t^{0.5}$ and q_t.

$$q_t = K_{id}^{t^{0.5}} + c \text{.....Eq. 1.18}$$

In the above equation, half-life is denoted by $t_{0.5}$, boundary thickness by C, rate constant of intra-particle diffusion by K_{id} and adsorption capacity at time t by q_t.

1.8. Efficiency of Nanoparticles in the Heavy Metal Removal

Nanomaterials have attracted significant attention for their ability to remove heavy metals from wastewater. They possess active groups, produce fewer flocculants, and have a large surface area. This makes them a promising option for addressing heavy metal pollution in terms of human health and the environment. Compared to previous sorbents, nanoparticles offer advantages such as recyclability and cost-effectiveness. However, their application on a larger scale is hindered by challenges in regenerating them and removing them from wastewater consistently. To overcome these issues, researchers are focusing on surface functionalization of nanoparticles using inorganic materials, carbon, biomolecules, and polymers. This Functionalization enhances the nanoparticles, adsorption capacity and facilitates their separation. It also improves their stability against oxidation and increases selectivity towards specific metal ions. Functionalization involves chemical bonding, complex formation, and ligand combination, along with Van der Waals and electrostatic interactions, which contribute to the adsorption selectivity of metal ions. Hydrophilic components like polyvinyl alcohol, polyvinyl pyrrolidone, and polyethylene glycol can be used as capping agents to coat the nanoparticles, preventing their agglomeration [24]. The surface-area-to-volume ratio of the nanoparticles is increased through functionalization, resulting in better dispersion in solution. The geometry array and choice of coating agents determine the surface areas and overall size of the nanoparticles, which are crucial for the selective and efficient adsorption of various metal ions from wastewater.

1.9. Research Studies on Adsorption by Forward Osmosis

In recent decade, the scientific community has worked on developing advanced membrane separation techniques for heavy metal removal from wastewater. Simultaneously, increasing water scarcity has put a stress on obtaining the freshwater from seawater through membrane separation technique.

A research study conducted by Cui et al. has demonstrated that forward osmosis is an effective technique for removal of heavy metals from wastewater. In this research, a novel forward osmosis (FO) membrane has been synthesized as thin film composite separating barrier. The draw solution for this was hydroacid complex (Na-Co-CA).

This TFC membrane is capable of removing variety of heavy metals such as Cu^{+2}, Cd^{+2}, Pb (II), Hg^{+2} and As while achieving 99.5% of removal efficiency. The rejection rate of forward osmosis is much greater than nanofilteration (NF). The heavy metal removal was increased by higher concentrations of draw solutions. Also, by increasing the concentration of heavy metals in feed solution the rejection rate was maintained at 99.5% [18].

In a research study conducted by He et al. a novel PDA/MOF-TFN membrane was synthesized by co-deposition. The main objective of using this TFN membrane for forward osmosis is to cater the barriers of poor stability, membrane loss and aggregation. When MOF-801 nanoparticles are added in PDA/MOF-TFN membrane, it has enhanced the salt rejection rate, water permeability and removal of heavy metals. It has increased the 30% of the water flux and decreased 44% of the reverse salt flux compared to the conventional TFN membranes. The PDA/MOF-TFN membrane showed greater capability of heavy metal removal for Pb (II), Cd^{+2} and Ni^{+2} [25].

For improving the diffusion of salts and rejection of heavy metals through thin film composite membrane forward osmosis layer of bovine serum albumin (BSA) incorporated on polyamide (PA) active layer was synthesized supported on glass nanofiber layer. The polyamide layer increased the salt diffusion and increased the heavy metal rejection by giving swellable water channels. The large porosity and pore size of the glass nanofiber layer assisted flow process, channels, increased internal concentration polarization and enhanced water flux for removal of heavy metals [25].

Alireza Saeedi-Jurkuyeh et al. in their research study analyzed the effect of concentration of active layer material on heavy metal rejection rate for improving the forward osmosis (FO) performance. They also increased the concentration of draw solution ions for increasing the process efficiency. The Thin film nanocomposite material was graphene oxide composited with polyethylene glycol. The TFN membrane showed increased hydrophilicity, water permeability and heavy metal rejection rate [24].

There is a need of in-depth and multi-dimensional research in forward osmosis for accomplishing adsorption of heavy metals through thin film nanocomposite

membranes. As an innovative technique, forward osmosis (FO) holds a great potential for handling the heavy metal contamination in environment.

1.10. Overview of Graphene and Reduced Graphene Oxide (rGO)

Since 2004, graphene as a unique 2-D material has attracted great attention. It is made up of single carbon atoms layer in hexagonal lattice arrangement which makes it distinct than the traditional materials. Despite possessing thin structure, graphene shows exceptional strength, electrical and thermal conductivity and good surface area. These characteristics has widened the application of graphene in various research fields i.e., sensors, composites, electronics and energy storage equipment. Reduced graphene oxide is a modified form of graphene which possess a great potential in many applications. There are many oxygen-containing functional groups on the surface of graphene oxide (GO) as it is synthesized through oxidation of graphite. These oxygen-containing functional groups make graphene oxide (GO) hydrophilic and soluble in different solvents. By reduction of GO, reduced graphene oxide (rGO) is synthesized which has partial graphene-like structure and some of its oxygen atoms removed. rGO has high mechanical strength, surface area and electrical conductivity as graphene oxide (GO), however due to functional groups rGO is a unique material for adsorption applications [26].

1.10.1. Properties of Reduced Graphene Oxide (rGO)

Due to rGO's distinct composition and structure it has attained significant attention in adsorption systems. rGO is synthesized by graphene oxide (GO) which is made by oxidation of graphite. There is single carbon lattice GO with different oxygen-bearing functional groups on its surface such as carboxyls, epoxides and hydroxyls etc. When GO is reduced in rGO, some of the oxygen-containing functional groups are removed while reforming the pristine like structure of graphene. The electrical conductivity in rGO increases due to decreased amount of oxygen and increased sp^2 carbon-carbon bonding. Based on the reduction process applied, the properties and structure of rGO can change. The reduction extend and structural characteristics of rGO can be analyzed by different characterization techniques i.e. Fourier-transform infrared spectroscopy (FTIR), X-ray diffraction (XRD) and scanning electron microscopy (SEM) [27].

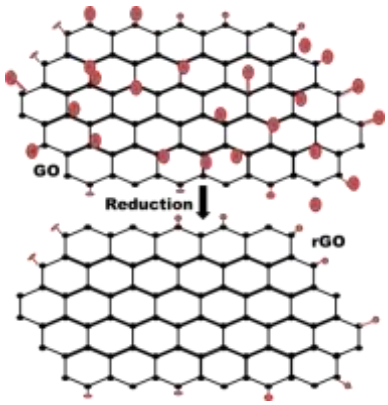

Figure 9: Reduction of GO into rGO

1.10.2. Unique Characteristics and Advantages as an Adsorbent

rGO is a distinctive material due to its large surface area, porosity, conductivity and good chemical stability. rGO possess greater number of active sites on its 2-D structure which increases the specific surface area. Presence of pores render higher surface area and accommodation space for more number of adsorbate molecules. rGO is much more chemically stable than GO due to lesser number of oxygen-containing functional groups and sp^2 carbon structure. rGO shows unique mechanical strength during adsorption due to its inherent structural strength. These unique properties make rGO a suitable adsorbent for vast array of pollutants.

1.10.3. Synthesis Methods of rGO for Adsorption Applications

There are many methods to synthesize GO most commonly used synthesis methods are Hummer's and Staudenmaier methods. After the synthesis, GO is reduced in rGO by chemical, thermal and electrochemical methods. The properties and efficiency of rGO depends on its synthesis route. Hummer's method show higher degree of oxidation and more defects can be resulted by strong oxidation agents and extreme reaction conditions. However, Staudenmaier method is moderate and result in partial reduction of graphite into GO. After synthesis of GO, it is reduced into rGO by thermal, chemical and electrochemical processes. In thermal reduction, GO is subjected to high temperature ensuring inert atmosphere. In chemical reduction, chemical agents are used for reduction of GO into rGO. Chemical agents used commonly are ascorbic acid, sodium borohydride and hydrazine. Reduction of GO through electrochemical pathway require electrochemical cell. GO acts as a working electrode working for reduction process.

1.10.4. Adsorption Mechanisms of rGO

It is extremely important to understand the adsorption mechanism of reduced graphene oxide (rGO) for analyzing the adsorption effectiveness of it in different applications. There are different mechanisms of adsorption on the surface of rGO resulting in greater adsorption specificity and capacity[28]. The mechanism of adsorption for rGO are physisorption, chemisorption, π-π and electrostatic interactions. physical adsorption happens through weak Van der Waal forces formed with adsorbate molecules. In chemical adsorption or chemisorption, strong chemical interactions or bonds are formed between adsorbate molecules and rGO. There are a lot of aromatic rings in rGO due to which there are non-covalent interactions or stacking which is called π-π interactions. Different pH levels will encourage rGO to interact differently with charged adsorbates which establish the electrostatic interaction between rGO and asorbate's surface.

1.10.5. Applications of RGO as an Adsorbent

As an adsorbent, rGO (Reduced Graphene Oxide) has attained special interest due to its unique and multi-dimensional implementations in different fields. It is vastly applied in water purification for heavy metal, organic, and emerging pollutant removal. Other than this, it is used as absorbent for harmful gases in air such as CO_2, VOCs, NOx and SOz. Due to its unique properties it has been recently employed in drug delivery systems, for oil spill cleaning and superconductors.

1.10.6. Factors Affecting Adsorption Performance

There are different factors which can affect the adsorption capability of Reduced Graphene Oxide (rGO) by altering its contact with adsorbates. Comprehending these factors is important for enhancing rGO's performance in various applications. Physiochemical properties of rGO such as porosity, charge distribution, large surface are and functional groups affect specificity and adsorption capacity of rGO. Adsorbate-specific factors such as concentration, molecular size, solubility have an influence on rGO's performance as an adsorbent. The interaction of adsorbate and adsorbent material can be highly affected by temperature, pH and ionic strength. There are many factors which affect the commercial application of rGO as an adsorbent. When there are competing substances in a medium, they fight to occupy the available active sites which can adversely affect the adsorption capacity of rGO.

Scalability of rGO synthesis is one of the main obstacles in real-time application. The commercial application of rGO is limited as yield of production methods is in small amount. The commercial application of rGO in adsorption is non-viable due to cost-ineffectiveness. The raw material required for graphene synthesis are highly expensive which affects the expenditure for rGO synthesis.

Comprehending the ability of rGO in complicated environmental matrices. In the controlled laboratory environment, rGO shows good adsorption efficiency though, in practical scenarios, the workability of rGO will be different as the mechanisms will be affected by different environmental conditions such as co-existing substances, pH and mixture of pollutants. The selectivity of rGO-based adsorbents can be increased by altering the surface functionalities. Adsorption ability of rGO can be enhanced by conjugating it with other materials i.e. zeolites, polymers and nanoparticles [29].

1.10.7. Research Studies on Application of rGO in Desalination

Due to increasing global need of fresh water, more research efforts are focused on devising effective and sustainable desalination methods. Among these efforts, reduced graphene oxide (rGO) is a promising candidate for seawater desalination. Unique characteristics of rGO such as mechanical strength, large surface area, and high electrical conductivity of rGO have enabled the application of it in desalination and adsorption. There are many recent researches which are addressing scientific efforts for employing rGO for desalination by forward osmosis.

Deka et al. in their research efforts have fabricated rGO membrane supported on nylon and doped with polystyrene sulfonic acid. They have employed it for desalination by forward osmosis. The results have shown that rGO/PSS membrane possess great potential for desalination. The membrane has shown a good water flux of 34 LMH with salt flux of 0.18 g/L [25].

Shawky, (2020) has compared graphene oxide GO-TFC, rGO-TFC, and carbon nanotubes membranes for desalination by forward osmosis. They have focused on increasing the water permeability of the nanocomposite membranes. The membranes fabricated with rGO-TFN have shown a good water flux of 24 LMH. Besides this, water permeability through the membrane has also increased by the incorporation of rGO in TFC membranes [25].

Fan et al., (2019) have fabricated novel rGO/nanocarbon hollow fiber membrane for achieving maximum forward osmosis in desalination. The results have shown high

performance with water flux of 22.6 LMH. The membrane has also shown lesser reverse solute flux showing minimum concentration polarization.

Romaniak et al., (2021) have synthesized thin graphene oxide (GO) and reduced graphene oxide (rGO) desalination membranes and compared their performance. The results have shown that rGO membranes have shown better desalination performance. The adsorption of Na^+ and Cl^- depends on the extent of GO reduction. With the increase in the reduction of graphene oxide, the ion blockage increases [30].

1.11. Layered Double hydroxide (LDH)

Layered double hydroxides (LDH) are a unique group of inorganic compounds which are also called hydrotalcite-like materials or anionic clays. It is a type of nanoparticle that is basically employed in catalytic applications. LDH has been renowned due to its cost-effectiveness, scalability, lesser toxicity, and stability. It is different and unique from other layered materials as different hybrid composites can be manufactured by it possessing distinctive characteristics such as memory effect, large surface area, shape-specific ion exchange, and catalytic performance in different fields [31].

1.11.1. Fundamentals of LDHs

LDHs have alike structure as hydrotalcite mineral-$[Mg_6Al_2(OH)16]CO_3{\cdot}4H_2O$, first discovered in 1842. In 1942, Feithnecht synthesized first layered double hydroxide and named those double sheet structures. The structural features of layered double hydroxide (LDH) was first studied by Allmann in 1960s by X-ray diffraction (XRD). LDH are 2-D anionic thin layered compounds which has metal hydroxide ions arranged in octahedral space creating brucite-like structure. $(M^{2+})_{1-x}(M^{3+})_x(OH)^2.A^{n-x}/n.zH_2O$ is a general formula for LDH in which M^{+3} is metal cation in valency III state, M^{2+} metal ion in II valence state and A^{n-} denotes anion. In the layered structure, the positively charged ions form positive layer with charge density proportional to trivalent metal ratio x which is equal to M^{2+} and ranges from 0.2-0.33. In the interlayers, anionic species are present with water molecules contributing to stability of LDH [32]. There are distinctive characteristics of LDH i.e., anion mobility, base surface and as there is positive charge on the layers, anion exchange is favourable. By employing anion exchange method, water molecules and anionic species trapped in interlayers can be exchanged with desired anions. On calcination, LDH forms composite metal oxides which have excellent catalytic abilities. Memory

effect and reconstruction ability is another distinctive characteristic of LDHs. Hydroxides decompose at high temperatures and given metal oxides are treated with suitable anions. Magnetic properties of LDH can be changed by addition of organic anions layer [33].

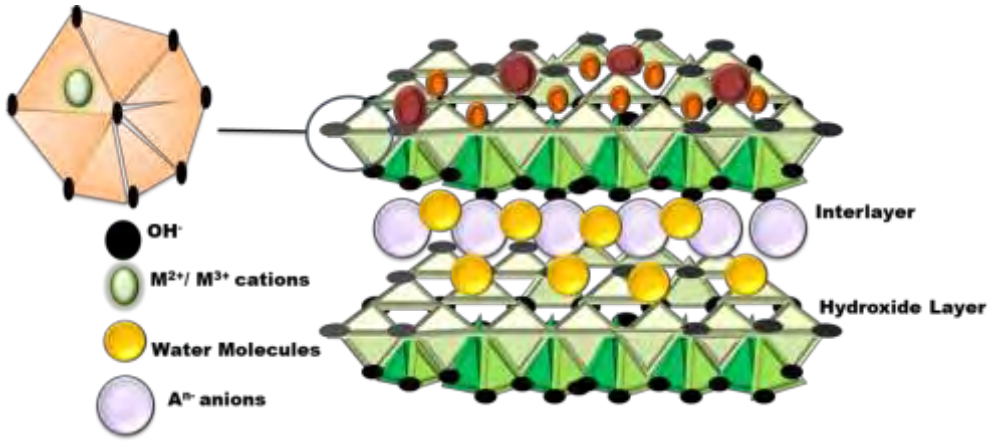

Figure 10: Structure of Layered Double Hydroxoide (LDH)

1.11.2. Methods for LDH Synthesis

There are various methods for synthesis of LDH by different metal divalent and trivalent ions. As LDH is a complex compound and have different associated phases, it is required to give controlled size and composition to its compounds. Main and widely used synthesis methods are summarized in the table.

Table 1: Synthesis methods for Layered Double Hydroxides (LDHs)

Method	Working Principle	Advantages	Drawbacks
Co-precipitation Method	In this method metal cations and anions are precipitated simultaneously	Rapid and easy	Uncontrollable layer growth
Ion Exchange Method	Interlayer anions are exchanged with desired ionic species.	Easy and versatile. High intercalation performance	Limitation of precursor
Hydrothermal Method	In this method, high temperature and pressure is given to the aqueous solution.	Tailored size and composition	Lengthy synthesis time
Sol-gel Method	In this method, precursors underGO hydrolysis, and gel is formed in solution.	Thorough mixing Desired structures and composition Symmetrical coating	Complicated and time consuming Agglomeration

1.11.3.Applications of Layered Double Hydroxide (LDH)

The unique properties of LDH have allowed researchers to use it in a wide variety of scientific, environmental and industrial applications. Due to their distinctive layered structure and adaptable interlayer chemistry, LDH has captured the attention of the scientific community for catalysis and environmental remediation.

Researchers are exploring the potential of layered double hydroxide (LDHs) to carry out seawater desalination. LDH has been proven an excellent candidate for catering to global water scarcity due to its adsorption and ion exchange capability. LDH can capture specific ions from water due to their selective intercalating ability thus, it can contribute to economical and energy-efficient seawater desalination. Capacitive deionization is a new desalination technique in which an electric field is applied to capture specific ions from water. The high regeneration ability and surface area of LDH make them a suitable candidate for this technique while reducing energy consumption and environmental impact.

Mojtaba Bagherzadeh et al. have employed novel WS_2/CuAl LDH nanosheets incorporated with TFC membrane for improved desalination through forward osmosis. These membranes have shown good desalination efficiency along with high water flux i.e., 0.42 g/l and antifouling properties [32].

Lei et al. have used CoFe-LDH/MXene membrane as a Cl^{-1} electrode in capacitive deionization. The results of this study have shown that CoFe-LDH/MXene membrane is tough leading to their self-stability. Besides, good stability it has shown a good desalination efficiency of 149.25 mgg^{-1} [33].

For desalination, the potential of LDH material still needs to be explored. This research has employed a novel LDH nanocomposite NiMoV LDH with rGO to achieve simultaneous desalination and heavy metal adsorption.

1.12. Problem Statement

Freshwater scarcity is a pressing and escalating problem globally. This water scarcity is increasing due to population growth, pollution, and global warming. Seawater constitutes 97% of the total Earth's surface. Freshwater can be obtained by enhanced desalination of seawater which can be used for drinking and consumption purposes. There are many conventional desalination methods (such as distillation, RO and

electrodialysis) but all of them are energy-intensive i.e., need a lot of thermal and electrical energy which makes them unviable. Besides accomplishing desalination, heavy metal pollution is also a burning issue for water quality. Thus, there is a need to develop a cost-effective and energy-efficient treatment method for simultaneous desalination and heavy metal removal.

1.13. Aims and Objectives of the Study

The goal of this study is to achieve simultaneous desalination and heavy metal removal from water using forward osmosis. To accomplish this goal following objectives are considered

- To fabricate of rGO/NiMoV LDH thin-film composite membranes supported on cellulose acetate.
- To construct different ratios i.e. 3%, 7%, and 10% of rGO/NiMoV LDH membranes with varying wt% of rGO.
- To achieve maximum desalination and adsorption of lead Pb (II) (heavy metal).
- To achieve a good water flux and minimum reverse solute flux.

2. EXPERIMENTAL METHODS

This chapter aims at explaining the materials and experimental method being followed in this research study. Hydrothermal method is used to synthesize the composite for this study which is rGO/NiMoV LDH. Moreover, this section gives an overview of the tests applied for obtaining the results for desalination and adsorption.

2.1. Methodology

2.1.1. Materials

Sodium Molybdate (Na_2MoO_4), Hydrochloric acid (HCl), Ethanol (C_2H_5OH), Nickel chloride hexahydrate ($NiCl_2 \cdot 6H_2O$), Urea ($CO(NH_2)_2$), synthetic graphite, potassium permanganate ($KMnO_4$), sulphuric acid (H_2SO_4), hydrogen peroxide (H_2O_2), NH_3 solution and hydrochloric acid (HCl), ascorbic acid ($C_6H_8O_6$) and cellulose acetate membranes.

2.1.2. Synthesis of NiMoV LDH

1.2 mol of $NiCl_2 \cdot 6H_2O$, 0.4 mol of VCl_3, 5 mol of Urea ($CO(NH_2)_2$) were added separately in 50 ml of distilled water. It is stirred uniformly on a magnetic stirrer until it makes a homogeneous and dispersed solution. Then the solution was autoclaved at 120 ^{o}C for 12 hrs. The composite suspension was washed with distilled water and ethanol. The obtained composite was subjected to air drying for one day [34].

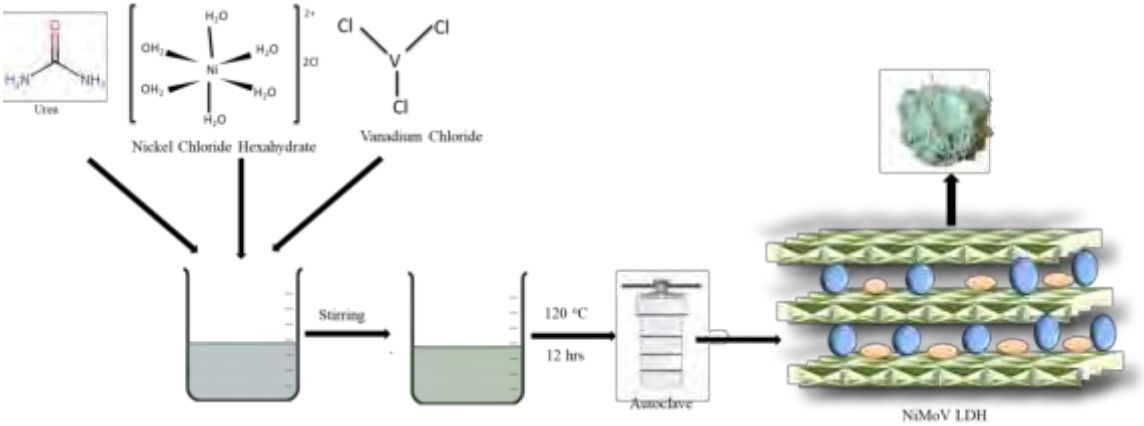

Figure 11: Synthesis of NiMoV LDH

2.1.3. Synthesis of GO

The graphene oxide GO was obtained by Hummer's method from synthetic graphite. Following this procedure, 3 ml of phosphoric acid (H_3PO_4) and 27 ml of sulphuric acid (H_2SO_4) in a volume ratio of 9:1 were added and stirred for a few minutes. Under stirring conditions, 0.225 g of powdered graphene was added in the mixing solution. Then 1.32 g of potassium permanganate ($KMnO_4$) was gradually added to the solution. The mixture was subjected to continuous stirring until it turned dark green. For removing extra $KMnO_4$, 0.675 ml of hydrogen peroxide (H_2O_2) was added drop-wise and stirred for 10 minutes. Solution was cooled as an exothermic reaction occurred. 30 ml of deionized water (DIW) and 10 ml of hydrochloric acid (HCl) was added in the solution and it was centrifuged for 7 minutes at 5000 rpm. The supernatant was discarded and residues were washed 3 times again with DI water and HCl. The washed GO suspension was subjected to oven drying at 90 ^oC for 24 hrs. The obtained powder is pure GO[35].

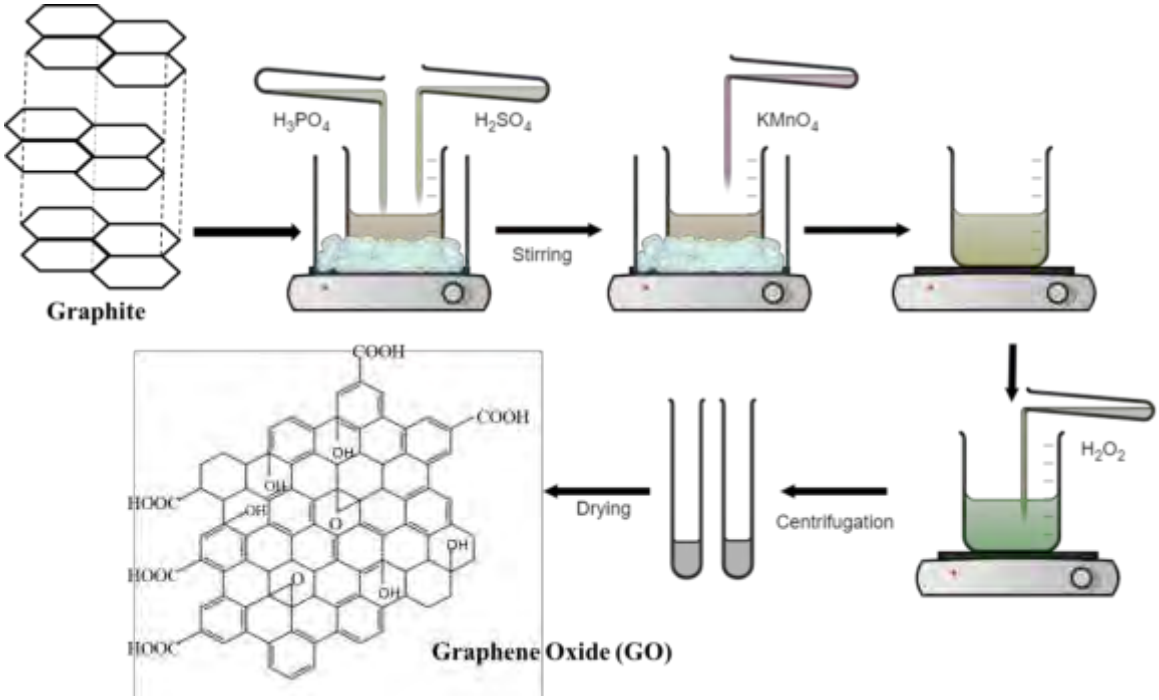

Figure 12: Synthesis of GO

2.1.4. Reduction of Graphene oxide (GO)

A suspension of GO (0.1 mg/ml) was prepared by sonicating dried GO in distilled water. To its 100 ml, 100 mg of ascorbic acid was added. The pH of the medium was adjusted to ~10 by adding NH_3 solution to promote colloidal stability through the

electrostatic repulsion. The mixture was allowed to stir at 65℃ and samples were withdrawn at 10 minutes' intervals until 1 hour.

A GO suspension was made with concentration 0.1mg/ml by sonicating the dried GO in distilled water. In 100 ml of this solution, 100 mg of ascorbic acid was added. The pH of the solution was adjusted at 10 by addition of NH_3 for encouraging the colloidal stability by electrostatic repulsion. The solution was continuously stirred for 1 hour at 65 ^oC. The solution was then subjected to centrifugation at 7000 rpm for 7 minutes. Supernatant was discarded and residual suspension was dried in the oven at 50 ^oC to 60 ^oC for 15 hours [27].

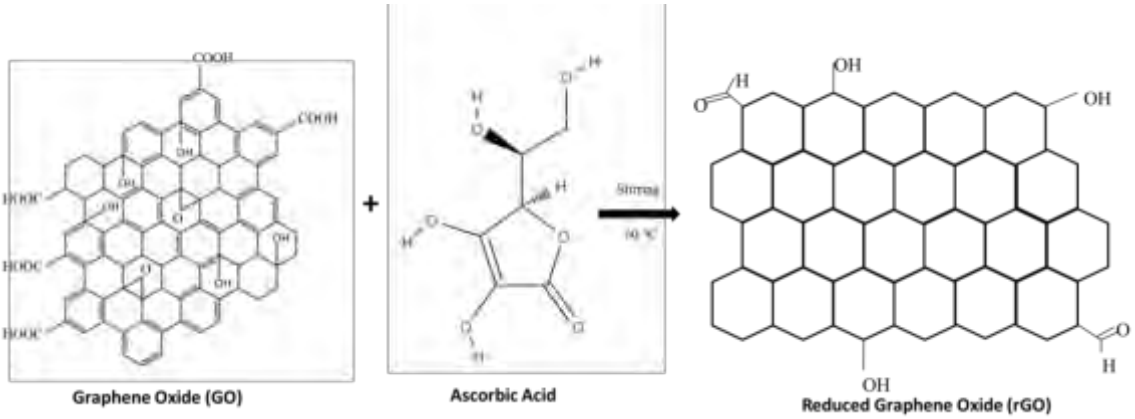

Figure 13: Reduction of GO into rGO

2.1.5. Synthesis of NiMoV LDH/rGO Composite

According to the composite wt. percentages 3%, 7% and 10% of rGO, NiMoV LDH LDH and rGO were measured. 3%, 7% and 10% of rGO was dissolved in a separate beaker in 20% of ethylene glycol in distilled water. 3%, 7% and 10% of measured NiMoV LDH will be added 20% w/v of ethylene glycol in water in separate beakers. The solutions were sonicated and stirred for 2 hours. After 2 hours, the solutions were mixed i.e., 3% rGO was mixed in 3% NiMoV LDH solution. The solutions were again stirred for 1 hour. After 1 hour, the solution was autoclaved at 120 ^oC for 12 hours. Then the solutions were washed with distilled water two times and with ethanol three times and air dried [27].

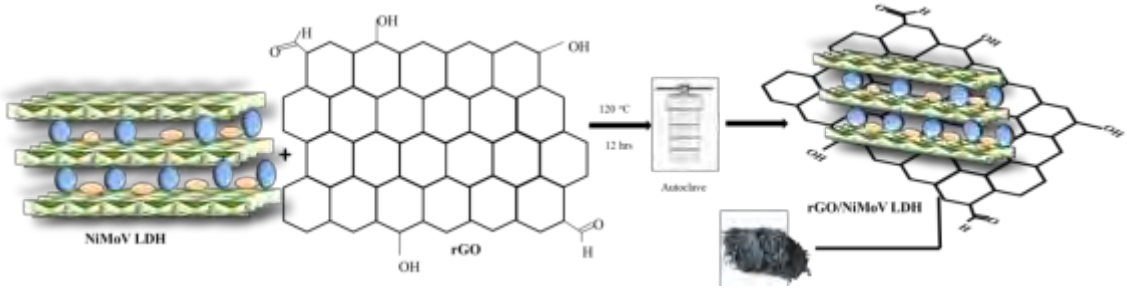

Figure 14: Synthesis of rGO/NiMoV LDH by hydrothermal method

2.1.6. Membrane Fabrication

The composite membranes were fabricated by vacuum filtration. Cellulose acetate membranes were placed in vacuum assembly and a composite solution was filtered from it. Membranes were in concentration of 5mg, 10mg, 15mg and 25mg for each percentage. The membranes were dried in oven at 60 ^{o}C for 2 hours [36].

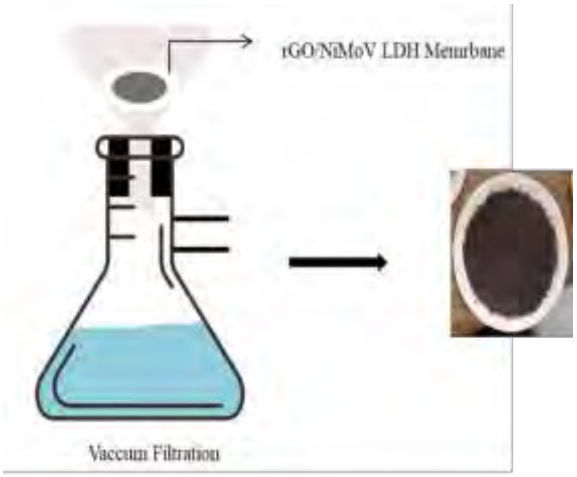

Figure 15: Membrane fabrication by vacuum assembly

2.2. Experimentation

2.2.1. Desalination Experimentations

The desalination experiments were done in a u-shaped tube in which a membrane was placed in the middle. The tube was filled with a feed solution of 1M salt solution from one side and 2M sucrose solution on the other side which is referred to as a draw solution. The pH of both solutions was maintained between 6-8. The membrane side loaded with composite was facing feed solution. Gradient for forward osmosis is created by sucrose draw solution. The changes in NaCl concentration in feed solution were noted by analyzing the changing conductivity. The samples were collected from feed and draw solutions over time. The samples were then analyzed by Mohr's method for calculating the concentration of Cl^- ions in feed and draw solutions.

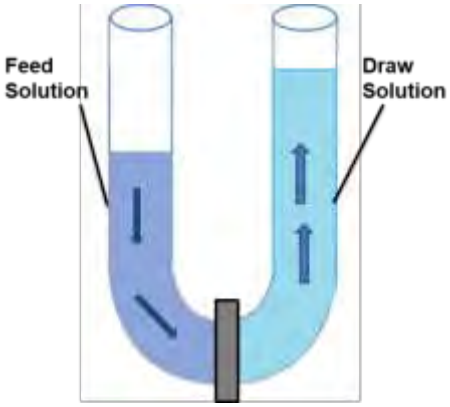

Figure 16: Desalination Set-up

2.2.2. Salt Rejection Rate

The membrane separation performance for NaCl was done by calculating salt rejection rate by following equation. Where R_s is salt rejection rate, C_f is salt concentration in feed solution and C_d is salt concentration in draw solution [37].

$$R_s\,(\%) = \frac{Cf - Cd}{Cf} \times 100 \text{.....} \textbf{Eq. 2.1}$$

2.2.3. Water Flux

Water flux of the membrane gives information about the volume of water that can pass through a particular area of membrane in a particular time period. Water flux of rGO/NiMoV LDH composite membranes was calculated by gravity assisted filtration. The equation for measuring water flux is as follows [38]:

$$J_w\,(L\ m^{-2}\ h^{-1}) = \frac{V}{A\,x\,t} \text{.....} \textbf{Eq. 2.2}$$

2.2.4. Rejected Solute flux

Rejected solute flux, also called retentate flux, is the rate at which the dissolved ions are rejected by the semi-permeable membrane during filtration. The rejected solute flux for synthesized composite membranes is calculated by following equation [31]:

$$J_s\,(mg\ L^{-1}\ m^{-2}\ h^{-1}) = \frac{\Delta\ Ct\ Vt}{Am\ \Delta t} \text{... ... ...} \textbf{Eq. 2.3}$$

2.2.5. Adsorption of Lead (Pb (II))

The adsorption experiments were carried out in a batch.40 ppm stock solution for Pb (II) was prepared for analyzing the effect of composite dose. Four different concentrations of composites (5 mg, 10 mg, 15 mg and 25 mg) were dissolved in different falcon tubes containing 30 mL of Pb (II) solution in it. The samples were

collected after every 15 minutes which were then filtered and analyzed by atomic absorption spectroscopy. For analyzing the effect of pH, three 40 ppm solutions of Pb (II) were prepared. The pH values of these solutions were set at 6, 7 and 8. Then three of the composites i.e. 3%, 7% and 10% rGO/NiMoV LDH were added and the solution. These solutions were continuously stirred and samples were collected over a time period of 60 minutes. For analyzing the effect of pollutant dose, a composite having best removal efficiency was chosen. Different Pb (II) solutions with concentrations 10ppm, 20 ppm, 40 ppm and 100 ppm were prepared. Measured composite was added in the falcon tube with 30 mL Pb (II) solution. The falcon tubes were stirred continuously on the shaker. Samples were taken after every 15 minutes until the end of the experiment. All adsorption samples were analyzed by atomic absorption spectroscopy (AAS).

2.3. Removal Efficiency

For measuring the removal efficiency or percentage of Pb (II) ions, following equation was used [39]:

$$\text{Removal Efficiency (\%)} = \frac{\mathbf{Cf - Ci}}{\mathbf{Cf}} \text{ x } 100 \ldots\ldots\ldots\ldots\ldots\ldots \textbf{Eq. 2.4}$$

2.4. Adsorption Capacity

Adsorption capacity is ability of the adsorbent to adsorb maximum amount of adsorbate with it. It is calculated in terms of volume per unit mass of the adsorbent. The adsorption capacity of the composites was calculated by following equation [39]:

$$q_e \text{ (mg g}^{-1}\text{ L)} = \frac{\mathbf{Ci - Ce}}{\boldsymbol{W}} \text{ x V} \ldots\ldots\ldots\ldots\ldots\ldots\ldots\ldots \textbf{Eq. 2.5}$$

2.5. Simultaneous Adsorption and Desalination

The composite showing highest adsorbent efficiency and salt rejection was selected for carrying out simultaneous adsorption and desalination. The experiment was performed in a U-shaped tube in which 2 M of sucrose solution was used to create forward osmosis gradient. 1M NaCl solution having 40 ppm Pb (II) concentration was made and poured on the feed solution side. The samples were collected over time until the experiment ended. The samples were analyzed for adsorption by atomic absorption spectroscopy (AAS) and desalination analysis was done by Mohr's method for measuring the concentration of Cl^- ions in feed and draw solution both.

2.5.1. Mohr's Method

Mohr's method is used to calculate the number of chloride ions (Cl^-) by $AgNO_3$ titration. The end point of $AgNO_3$ titration is when all the chloride ions react with silver to form silver chloride precipitate. The remaining chromate ions of potassium chromate indicator react with silver ions to form silver chromate resultantly in red-brown precipitates. This method can determine the chloride ions concentration in seawater, brackish water stream and river water samples.

For performing Mohr's titration, 10 mL of sample was taken in a conical flask and 1 mL of indicators was added in it. Then the sample was titrated by 0.1 mol L^{-1} $AgNO_3$ solution which was in burette until the end-point of red-brown precipitates was reached. The volume of $AgNO_3$ which was used for titrating the sample was noted. The concentration of chloride ions was determined by the following formula [40,41]:

$$Cl^- \text{ (in g } L^{-1}) = V_{AgNO3} \text{ x } N_{AgNO3} \text{ x } M_{Cl-}/V_{sample} \quad \textbf{Eq. 2.6}$$

Where V_{AgNO3} is the volume of silver nitrate used, N is the normality of $AgNO_3$, M_{Cl-} is the molar mass of chloride ions in g mol^{-1} and V_{sample} is the volume of sample being titrated.

2.6. Atomic Absorption Spectroscopy (AAS)

Atomic absorption spectroscopy (AAS) is a technique which is used to analyze trace analytes by electrochemical atomization. It is a credible technique to determine the concentration of metals and metalloids in the sample. It is a simple and valid technique which can determine upto 62 metals. Besides determination, it also quantifies the metals in the sample.

2.6.1. Working Principle

AAS works on the principle of atomization of ground state atoms in the gaseous state by an atomizer which can absorb the radiation of specific frequency. AAS measures the absorption of atoms in ground state in their gaseous form. The ultraviolet light is absorbed by the atoms which promotes them to higher energy levels. The analyte is quantified by the amount of absorption. The instrument is calibrated with solutions of known concentrations to calculate the analyte concentrations by working curves [42].

3. EXPERIMENTAL TECHNIQUES

This chapter aims to explain the characterization techniques used to analyze the physiochemical properties of the synthesized material i.e., rGO/NiMoV. scanning electron microscopy (SEM), X-ray diffraction (XRD) and Fourier-transform Infrared Spectroscopy (FTIR).

3.1. Scanning Electron Microscopy (SEM)

Sizes, shapes, atoms arrangement and surface morphologies of materials are determined by scanning electron microscopy (SEM). In SEM, the monochromatic light beam is bombarded on the sample generating the signals which are detected by the detector. The signals which are generated give information about crystalline structure, morphology and chemical composition of the sample [43].

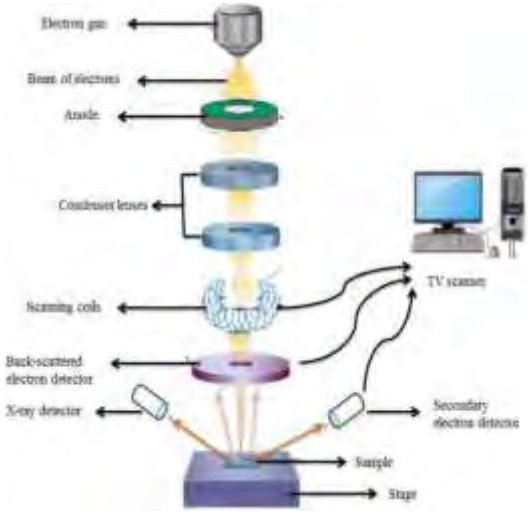

Figure 17: Working Principle of SEM

3.2. X-Ray Diffraction (XRD)

XRD is an advanced technique to determine the crystallographic properties of a material by identifying its crystalline structure. It is used to determine the thickness, density, thickness, cell dimension, sample purity and material phase identification.

3.2.1. Working Principle

The working principle of XRD is based on interaction between electrons of the sample material and x-rays. The sample is bombarded by a x-ray beam produced from a cathode ray tube. When the sample electrons and x-rays come in contact, a series of

interferences is produced. These interferences are based on Bragg's law which is as follows:

$$n\lambda = 2d \sin\theta \quad \text{.....Eq. 3.1}$$

In the above equation, λ is x-ray wavelength, d is the spacing between the rays, θ is the angle between scattering planes and incident rays and n is an integer [43].

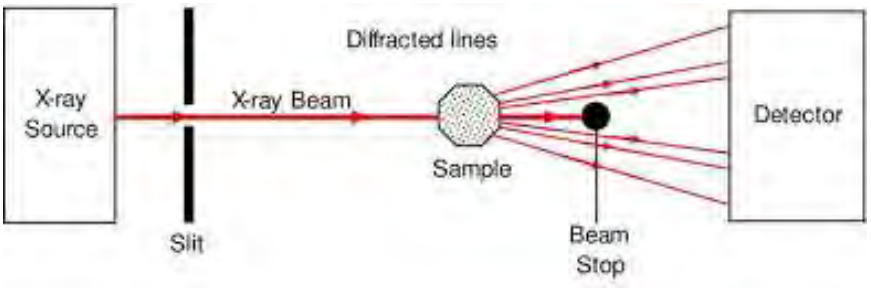

Figure 18: Working principle of XRD

3.3. Fourier-transform Infrared Spectroscopy (FTIR)

FTIR is an effective technique to determine the sample structure and composition by infrared radiations. The working principle of FTIR is that chemical bonds in the sample molecules absorb infrared radiations of specific frequency which give a characteristic spectra. By analyzing and interpreting these spectra impurities, chemical bonds and molecular properties of a sample can be determined [44].

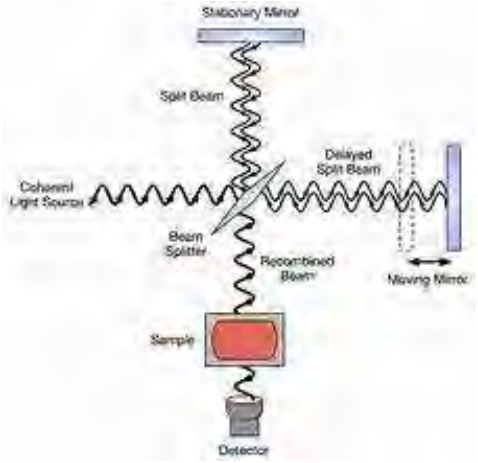

Figure 19: Working principle of FTIR

4. RESULTS AND DISCUSSION

This chapter focuses on all obtained results obtained from experimentation and characterization studies. The physiochemical properties of the synthesized composite membranes of different weights by percentage i.e. 3%, 7% and 10% rGO/NiMoV LDH were analyzed by scanning electron microscopy (SEM), X-ray Diffraction (XRD) and Fourier-transform infrared spectroscopy (FTIR). For measuring the adsorption of lead (Pb (II)), atomic absorption spectroscopy was used. For conducting desalination analysis, Mohr's method was applied.

For SEM analysis, the membrane was measured and cut to fit in the sample holder. It was then chemically fixed by formaldehyde followed by dehydration, drying and coating with some conductive material i.e. gold or platinum to reduce charging effects. For XRD analysis, the composite was grinded and dried. Then it was packed in the sample holder made of quartz. The holder was gently tapped to level the composite surface. XRD analysis was done by directing the X-Rays to the composite surface and diffracted X-Rays were measured. For sample preparation of FTIR, KBr pellets were made by mixing the finely powdered composite with potassium bromide (infrared transparent material). The analysis is done by passing infrared radiations through this pellet which analyzed the molecular vibrations. The spectrum was generated by infrared light's absorbance or transmittance.

4.1. Physicochemical Properties

Figure 19 shows the physicochemical properties of rGO/NiMoV composite membrane on cellulose acetate substrate. The SEM image reveals that the pore size of the membrane is 0.1μm and the particle size of the composite particles is 1 μm. The cross-sectional image of the membrane shows the layer of rGO/NiMoV composite on cellulose acetate membrane. The membrane surface is high microporous having spider-web like appearance which demonstrates its suitability for the filteration process.

The XPS analysis of the composite material confirms the presence of atoms such as Ni, Mo, V, O, C and P which confirm the chemical composition of the synthesized membrane material. Presence of phosprous is due to pH adjustment of the rGO

solution by Phosphoric acid. Whereas, there is a small amount of carbon in the composite as due to less proportion of rGO in the composite.

The FTIR peaks are showing presence of different functional groups in rGO/NiMoV composite. The peak at 600 cm^{-1} is related to M-O functional group which is between Ni-O in NiMoV LDH. The functional groups such as C-O (1000 cm^{-1}), -COOH (1300 cm^{-1}) , C=H (1600 cm^{-1}), C-H (3000 cm^{-1}), O-H (3400 cm^{-1}) and –OH (3700 cm^{-1}) are confirmed by FTIR peaks.

The X-ray diffraction (XRD) peaks of NiMoV LDH and the composite rGO/NiMoV reveals crucial details about their crystal structures. In NiMoV LDH, the (022) peak indicates specific atomic planes' presence and orientation within the crystal lattice. Furthermore, the (131) peak informs about the arrangement of atoms, aiding in phase identification, while the (422) peak offers insights into structural characteristics. The (002) peak signifies interlayer spacing in the LDH structure.

Shifting to the rGO/NiMoV composite, the (011) peak suggests a specific orientation of the crystal lattice. The presence of the (022) peak, akin to NiMoV LDH, indicates the retention of its structure in the composite. The (131) peak reflects the arrangement of atoms within the composite, and the (331) peak provides insights into its structural complexity. Similarly, the (422) peak denotes specific crystallographic planes. Additionally, peaks at (440, 553, 751) offer detailed information on the composite's complex structural characteristics.

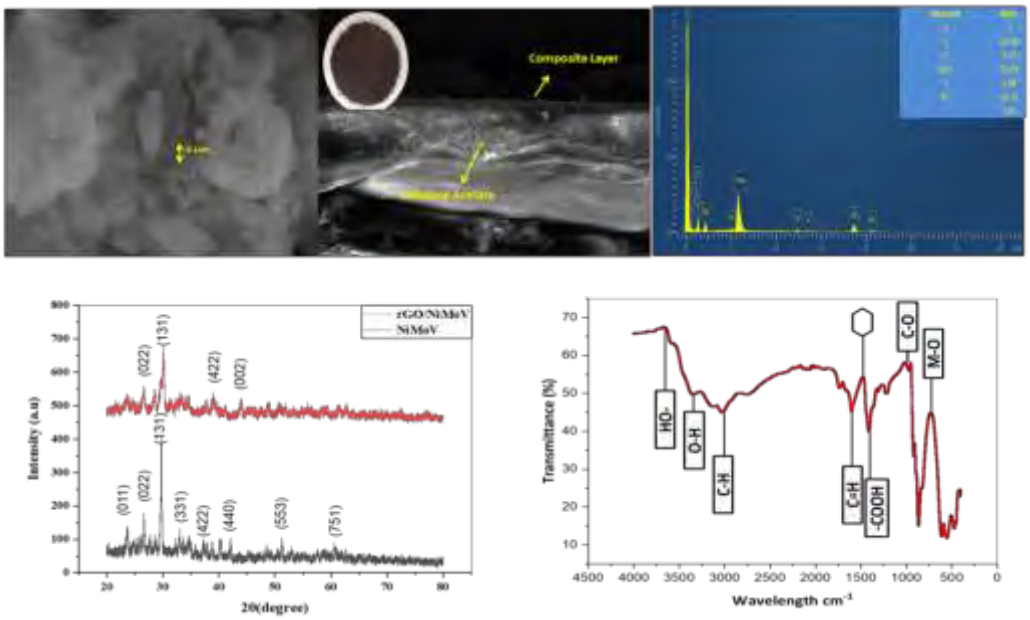

Figure 20: Physicochemical properties of rGO/NiMoV LDH

4.2. Adsorption Studies

4.2.1. Effect of Adsorbent Dose

Removal efficiencies of different doses i.e., 5mg, 10 mg, 15 mg, and 25 mg of rGO/NiMoV LDH composite (3%, 7%, and 10%) were calculated keeping the pollutant concentration at 40 ppm. The samples were analyzed with Atomic Absorption Spectrometry (AAS). The highest removal efficiency is achieved by 10mg of 10% rGO/NiMoV LDH. The hierarchy of Pb (II) removal efficiency for 3% rGO/NiMoV LDH is 5 mg > 25 mg >15 mg >10 mg, for 7% rGO/NiMoV LDH is 5 mg > 25 mg > 15 mg > 10 mg and for 10% rGO/NiMoV LDH is 10 mg > 15 mg > 25 mg > 5 mg. 10% of composite is having the highest percentage of rGO, which is an efficient adsorption for heavy metals. 10 mg of 10% rGO/NiMoV LDH is an optimum composite dose for complete adsorption of lead (Pb (II)). Whereas, 3% and 7% of rGO/NiMoV LDH are showing varying trends with composite dose. As the composite dose increases, the removal efficiency increases until a concentration where agglomeration of composite starts, decreasing the adsorption [20].

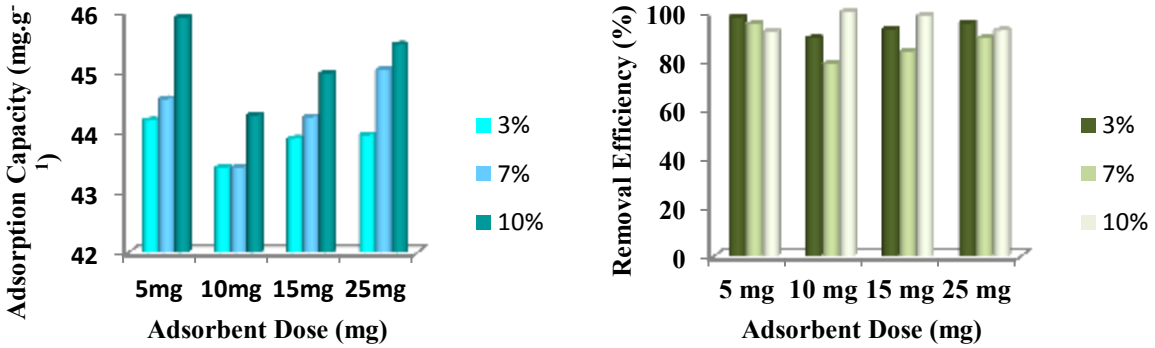

Figure 21: Removal efficiencies and adsorption capacities for adsorbent dose

The adsorption capacities of different composite doses were also calculated. 5 mg of each composite has highest adsorption capacities followed by 10 mg, 15 mg and 25 mg. It shows that 5 mg and 10 mg of composites doses possess highest ability to adsorb the Pb (II) ions with it.

Table 2: Removal efficiencies and adsorption capacities for adsorbent dose

Composite (rGO/NiMoVLDH)	Adsorption Capacity (mg g^{-1})				Removal Efficiency (%)			
	5 mg	10 mg	15 mg	25 mg	5 mg	10 mg	15 mg	25 mg
3%	44.19	43.41	43.89	43.95	97.77	89.17	92.83	95.38
7%	44.55	43.41	44.25	45.03	94.90	78.66	83.75	89.17
10%	45.90	44.28	44.97	45.45	91.87	100	98.40	92.35

4.2.2. Effect of Pollutant Dose

The effect of pollutant dose was analyzed on rGO/NiMoV LDH (3%, 7%, and 10%). The effect of pollutant dose was calculated at best-performing composite dose i.e. 10 mg. The pollutants doses were 10 ppm, 20 ppm, 40 ppm and 100 ppm. All composites showed maximum removal efficiency for all pollutant doses except for 100 ppm. The composites performed well until an optimum concentration of pollutant. 100 ppm is the saturation point of the composite where no more active sites are available for adsorption. The desorption effect occurs at higher pollutant concentrations which detaches the excess pollutant from the surface of adsorption [45].

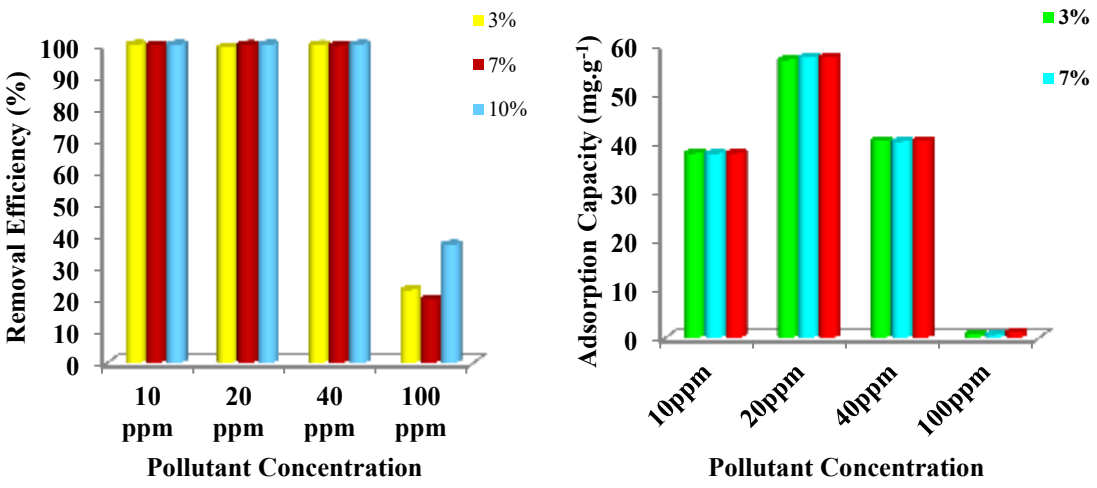

Figure 22: Removal Efficiencies and adsorption capacities for different pollutant concentrations

Table 3: Removal efficiencies and adsorption capacities for different pollutant concentrations

Composite (rGO/NiMoVLDH)	Adsorption Capacity (mg g^{-1})				Removal Efficiency (%)			
	10 ppm	20 ppm	40 ppm	100 ppm	10 ppm	20 ppm	40 ppm	100 ppm
3%	37.73	56.91	40.30	0.666	99.98	99.11	99.9	22.88
7%	37.65	57.37	40.17	0.582	99.76	99.92	99.62	20
10%	37.74	57.42	40.32	1.08	100	100	100	37.11

4.2.3. Effect of pH

The removal efficiency of 3%, 7% and 10% of rGO/NiMoV LDH composites at pH values 6, 7 and 8 were analyzed. It has been found that highest removal of Pb (II) is achieved at pH 6. At higher pH values, Pb (II) can be converted into $Pb(OH)_2$ and at lower pH values, the active sites of the adsorbents can be occupied by H^+ ions. Also the adsorption capacity calculations show that rGO/NiMoV LDH (3%, 7%, 10%) possess highest adsorption capacities at pH 6 [46].

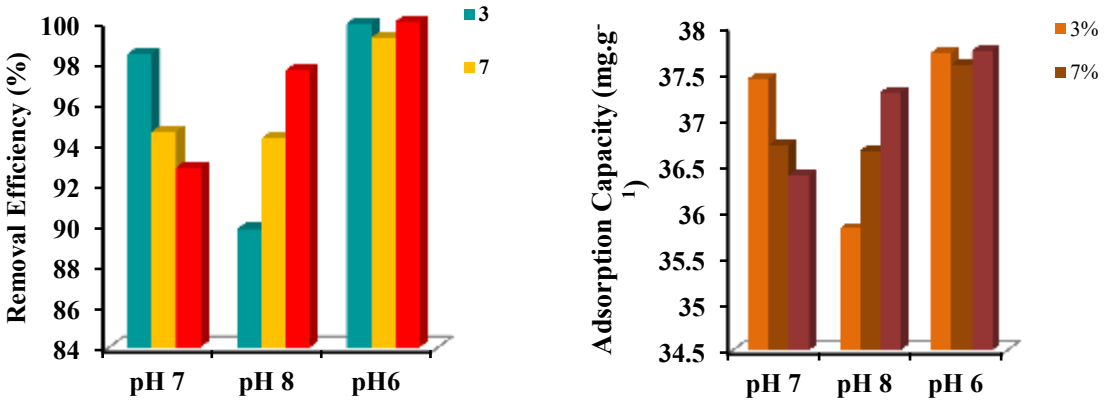

Figure 23: Removal efficiencies and adsorption capacities at different pH values

Table 4: Removal efficiencies and adsorption capacities at different pH values

Composite (rGO/NiMoVLDH)	Adsorption Capacity (mg g^{-1})			Removal Efficiency (%)		
	6	7	8	6	7	8
3%	37.72	37.44	35.82	98.40	89.80	99.90
7%	37.59	36.72	36.66	94.58	94.26	99.20
10%	37.74	36.39	37.29	92.83	97.61	100

Pzc determines the surface charge on the surface of the adsorbent, thus defines the nature of interaction between adsorbate and adsorbent. The Pzc of the rGO/NiMoV LDH is determined by salt addition method. The active sites are negatively charged when pH value is above Pzc and positively charged when pH value is lower than Pzc. For rGO/NiMoV LDH, Pzc value is 6 indicating the neutral surface charge on the active sites for adsorption of Pb (II). Thus, Pzc validates that appropriate pH for maximum adsorption of Pb(II) by rGO/NiMoV LDH is 6.

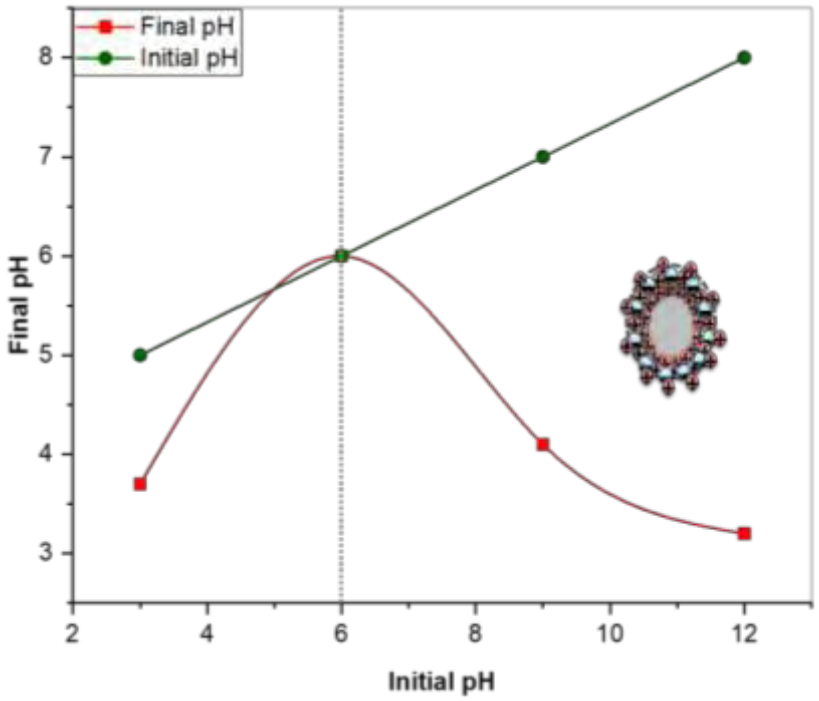

Figure 24: Point of zero charge for rGO/NiMoV LDH

4.2.4. Adsorption Isotherms and Kinetics

To study the interaction and mechanism of adsorption isotherms and kinetics are applied. The study is more consistent with Langmuir isotherm than Freundlich isotherm with R^2 value of 3% (0.998), 7% (0.997) and 10% (0.995). It infers that adsorbent has a homogenous surface with limited active sites on which adsorption occurs in monolayer. The maximum adsorption capacity according the Langmuir Linear model is 3% (37.41115 $mg.g^{-1}$), 7% (41.3736 $mg.g^{-1}$), and 10% (88.41733 $mg.g^{-1}$). It is evident that by increasing the weight proportion of rGO, Pb (II) adsorption increases. This shows enhanced chemical binding between active sites and Pb (II) ions. Moreover, K_L value of 1 indicates strong interaction of adsorbent and adsorbate surface. R_L which is dimensionless separating factors in Langmuir isotherm should be $0>R_L< 1$ ideally. The R_L factor for rGO/NiMoV LDH is 0.238095 which validates that physical adsorption is fitting.

The validation of Frendluich isotherm is carried out on the basis of n_F value. The ideal value of n_F should be between 1-10. The n_F values for 3% (3.533569 $mg.L^{-1}$), 7% (3.546099 $mg.L^{-1}$), 10% (3.521127 $mg.L^{-1}$) which demonstrates suitable chemical adsorption. The R^2 values for Frendluich isotherm are 3% (0.998), 7% (0.999) and 10% (0.999) which verifies heterogeneity of adsorbents. Higher K_F values of the adsorbent indicates that there is substantial chemical interaction between adsorbent and adsorbate surface due to presence of functional groups.

The concentrations limits for Langmuir and Frendluich isotherms are determined by Redlich-Peterson isotherm model. The R^2 value for Redlich-Peterson model is 0.99 which shows it an excellent fit with the experimental data. The β value for 3% and 10% is 0.7 and 7% is 0.1. It shows that anticipated isotherm is Langmuir.

The correlation factor R^2 for Temkin isotherm is 0.999, 0.998 and 0.964 for 3%, 7% and 10% of rGO/NiMoV LDH respectively. The adsorption heat B for 10% is the highest i.e., 1.71 Jol $mole^{-1}$. This increase in the adsorption heat is due to greater proportion of graphene as it possesses good thermal conductivity.

To determine the adsorption kinetics of the Pb (II) on rGO/NiMoV surface, pseudo-first order (PFO) and pseudo-second order (PSO) kinetics are applied on experimental data. Kinetics are important parameters to investigate the adsorption process and reaction sustainability. Table 1 summarizes

the values for PFO and PSO kinetics while validating their compatibility on the basis of R^2 values and adsorption capacity (q_e). Pseudo-second order kinetics is a suitable fit for all composites (3%, 7% and 10%) with superior R^2 value. Furthermore, the experimental and calculated adsorption capacities are well-collaborated with each other. It implies that the interaction between adsorbent and adsorbate surface is chemisorption via functional groups. Pb (II) is being adsorbed by chemical bonding with the functional groups present on rGO's surface.

Table 5 shows parameters for isotherm and kinetic modeling.

Table 5: Isotherm and kinetic modeling of rGO/NiMOV LDH

Kinetic/ Isotherm Model	Model Type	Parameters	3%	7%	10%
Langmuir	**Linear**	q_m (mg g^{-1})	37.415	41.376	88.417
		K_L	1	1	1
		R_L	0.238	0.238	0.238
		R^2	0.987	0.999	0.995
Freundlich	**Linear**	n_F	3.5339	3.54609	3.5217
		K_F (L . mg^{-1})	3323.8	3488.9	3370.6
		R^2	0.981	0.996	0.991
Redlich-Peterson	**Linear**	K_{RP}	0.295	0.0786	0.376
		A	3.542	3.515	3.380
		B	3.512486	3.481009	3.163873
		R^2	0.998	0.999	0.999
Temk	**Linear**	B ($Jmol^{-1}$)	0.969	2.529	1.714
		K_T ($L.mg^{-1}$)	0.02647	0.42705	0.06715
		R^2	0.9998	0.5712	0.76432
Pseudo-First Order Kinetics (PFO)	**Linear**	q_e (Cal)[b] (mg g^{-1})	3.68118	3.68858	3.67827
		$K_1 \times 10^2$ (min^{-1})	0.344	−0.288	-0.002
		R^2	0.997	0.992	0.977
Pseudo-Second Order Kinetics (PSO)	**Linear**	q_e (Exp)[a] (mg g^{-1})	10.95	8.05542	8.25228
		$t_{1/2}$ (min)	5.49	7.407	7.27
		h_0	0.09999	0.134	0.137
		q_e (Cal)[b] (mg g^{-1})	10.96	8.066	8.334
		$K_2 \times 10^2$ (g.mg^{-1} min^{-1})	0.000832	0.00207	0.00202
		R^2	0.998	0.997 0.996	0.996

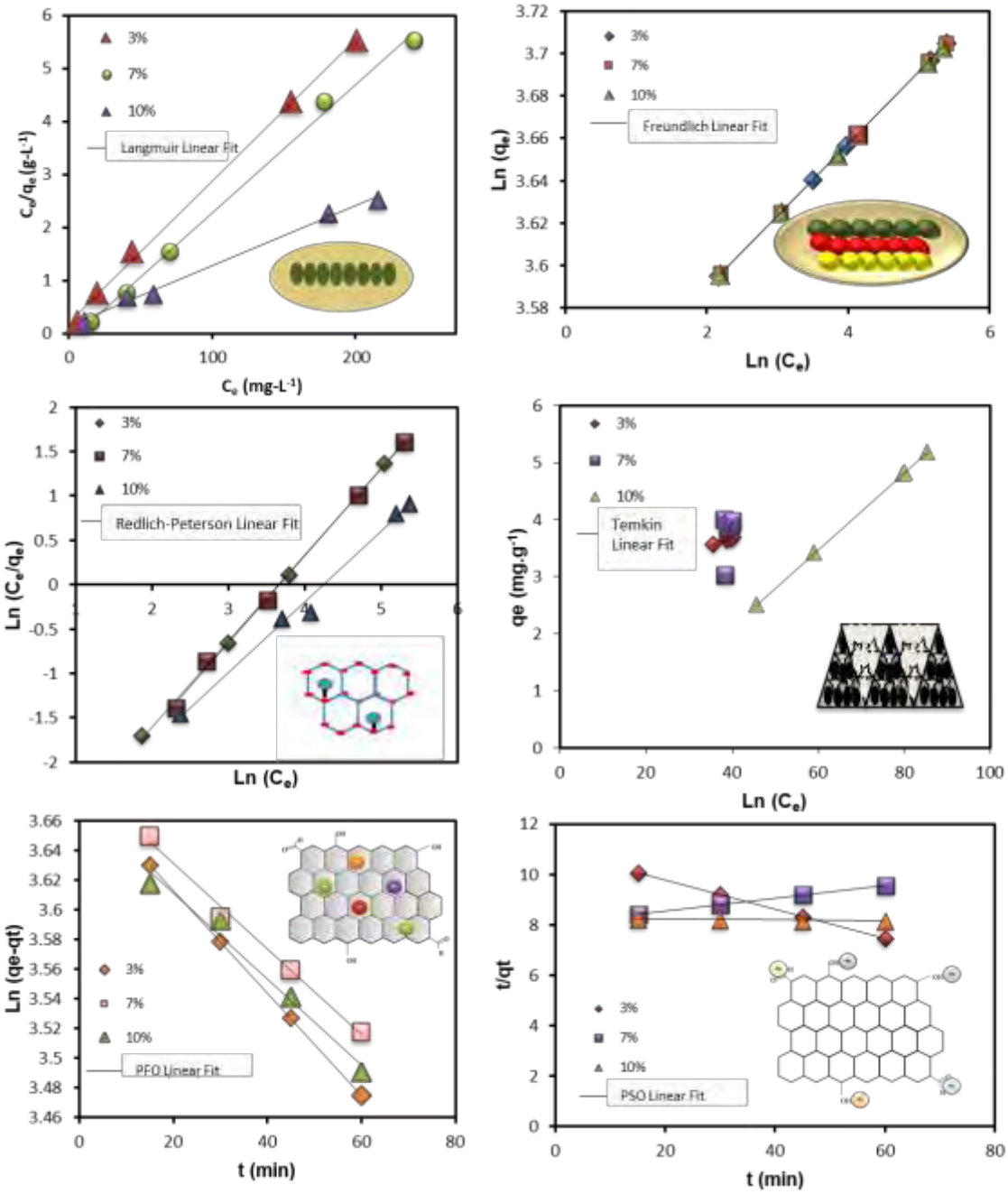

Figure 25: Kinetic and Isotherm modeling of adsorbent (rGO/NiMoVLDH)

4.3. Desalination Analysis

4.3.1. Salt Rejection Rate

The salt analysis of rGO/NiMoV LDH membranes was analyzed by Mohr's method. It has been investigated that 10mg of 10% rGO/NiMoV LDH composite showed highest salt rejection rate. Reduced graphene oxide (rGO) is an excellent adsorbent due to its large surface area, chemical stability, π-π stacking Interactions and functional groups i.e. carboxyl (-COOH), epoxy (-O-) and hydroxyl (-OH) groups[47].

As 10% rGO/NiMoV LDH is showing highest salt rejection rate, it shows that rGO is acting as a main physical adsorbent for Na^+ and Cl^- ions. Reduced graphene oxide (rGO) enhanced the stability and efficiency of the LDH membrane. The lowest salt rejection rate is shown by 3% rGO/NiMoV LDH due to lesser proportion of rGO by weight in the composite. Based on composite dose deposited on cellulose acetate membrane, 10mg of 3%, 7% and 10% rGO/NiMoV LDH has shown maximum salt rejection rate. Composite dose of 5 mg showed least salt rejection rate due to lesser number of available active sites on the composite. As the concentration of NPs increase the salt rejection rate also increases but to a certain concentration. The mechanism of NaCl removal is same as Pb (II) removal. 5 mg is a small composite dose on the membrane to provide appropriate number of active sites for Na^+ and Cl^- adsorption. Composite concentration is not directly linked with the salt rejection rate; it is the properties of the composite which affects the separation process.

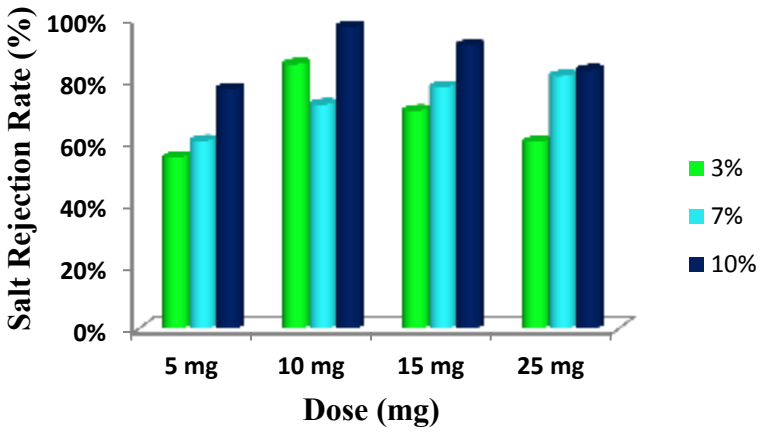

Figure 26: Salt rejection rate with composite dose

4.3.2. Water Flux

There are different factors by which the water flux of the membrane can be affected. These factors are; composite type, dose and membrane structure. The highest water flux is shown by 5 mg of composite dose whereas 25 mg has shown the least water flux. It means that in 25 mg of composite dose on membrane, lesser water volume passes through in more time. Whereas, in 5mg composite dose, more water volume passes through the membrane in lesser time period.

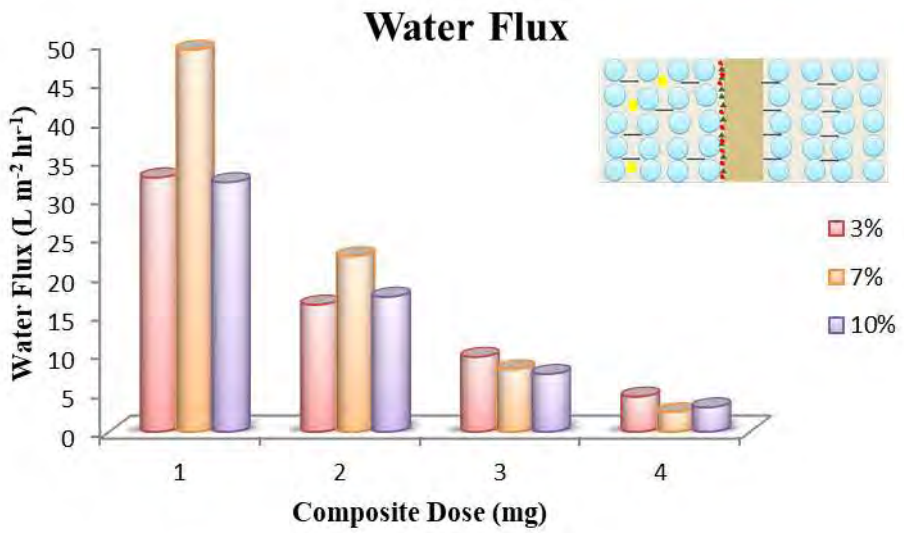

Figure 27: Water flux with composite dose

4.3.3. Reverse Solute Flux

The reverse solute flux of different membrane composite doses are shown in the figure below. The least reverse solute is of 10 mg of 3% rGO/NiMoV LDH. The maximum reverse solute flux is of 5 mg of 7% rGO/NiMoV LDH. There are different factors by which reverse solute flux of the membrane is affected. These factors are membrane properties, polarization, operating conditions and composite characteristics.

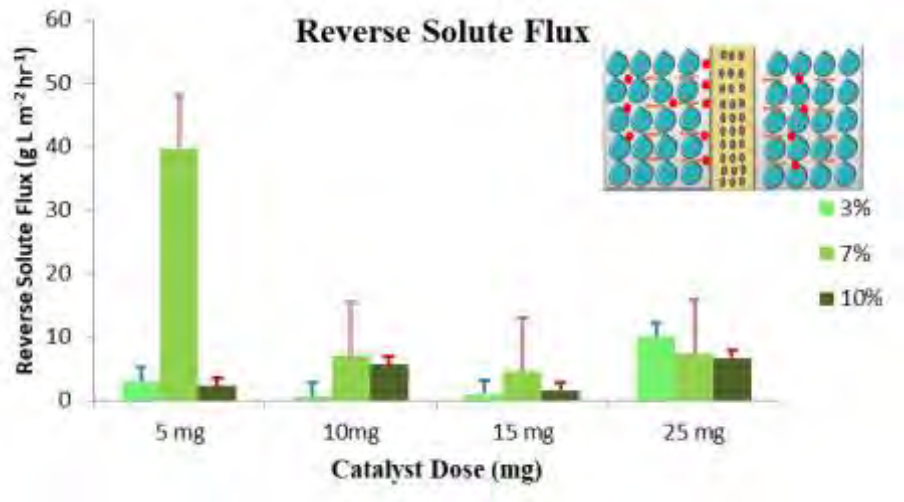

Figure 28: Reverse solute flux with composite dose

Table 6: Results of desalination study

Composite rGO/NiMoV LDH	Composite Dose (mg)	Salt Rejection Rate (%)	Water Flux (L m^{-2} hr^{-1})	Reverse Solute Flux (g L m^{-2} hr^{-1})
3% rGO/NiMoV LDH	5 mg	55%	32.6	3
	10 mg	85%	16.3	0.58
	15 mg	70%	9.6	1.1
	25 mg	60%	4.5	10
7% rGO/NiMoV LDH	5 mg	60.3%	49	39.7
	10 mg	72%	22.5	7
	15 mg	77.60%	8	4.6
	25 mg	81.20%	2.5	7.4
10% rGO/NiMoV LDH	5 mg	77%	32	2.26
	10 mg	97%	17.3	5.7
	15 mg	91%	7.4	1.6
	25 mg	83%	3.125	6.686

4.4. Simultaneous Desalination and Adsorption Study

For conducting simultaneous adsorption of Pb (II) and desalination by forward osmosis, composite showing highest efficiency was chosen. 10 mg of 10% rGO/NiMoV LDH has showed maximum adsorption efficiency along with salt rejection rate. The results of simultaneous study are written in the table below. The removal efficiency of Pb (II) and salt rejection rate is slightly lesser than the individual reactions (adsorption and desalination). It depicts that membrane has a limited number of active sites to adsorb the ions with it. Due to multiple number of ions i.e., Pb (II) , Na^+ and Cl^- adsorption sites are occupied. These ions are not chemically interfering with each other rather competing physically to attach with the active site. However, there is no effect of simultaneously performing the experiment on water flux and reverse solute flux. Following table displays the adsorption and desalination results:

Table 7: Results for simultaneous adsorption and desalination

Adsorption		Desalination		
Pb (II) Removal Efficiency	**Adsorption Capacity (mg g^{-1} L)**	**Salt Rejection Rate**	**Water Flux (L m^{-2} hr^{-1})**	**Reverse Solute Flux (g L m^{-2} hr^{-1})**
96.30%	6.85	97%	17.3	5.7

4.5. Removal Mechanism

The anticipated mechanism followed by rGO/NiMoV LDH for desalination and adsorption is due to graphene layers and interlayer spaces of LDH. The functional groups present on the surface of rGO chemically adsorb the Na^+ , Cl^- and Pb (II) ions by establishing electrostatic forces, complexion, π-π interaction and ion-dipole interactions. Layered Double Hydrooxide (LDH) has an anionic interlayer and above that there is a later of metal cations. The anionic layer can attract the positively charged ions whereas metals can attract the negatively charged ions towards it. Thus, it contributes to the adsorption of ionic species by intercalation and ion-exchange. This dual mechanism not only achieves Pb (II) adsorption but also enhances the water quality by removal of heavy metals and salinity.

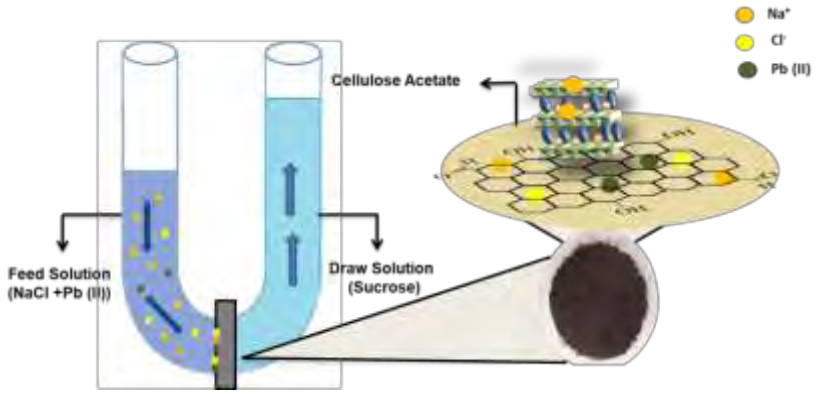

Figure 29: Anticipated mechanism of adsorption

5. CONCLUSION

This research study has successfully fabricated rGO/NiMoV LDH LDH membranes for achieving simultaneous desalination and adsorption of heavy metal Pb (II)). The nanocomposite is deposited on cellulose acetate support layer with 3%, 7% and 10% rGO/NiMoV LDH loadings (with varying wt% of rGO). The membrane having highest wt% of rGO i.e., 10% rGO/NiMoV LDH LDH showed maximum desalination and adsorption efficiency than 3% and 7% membranes. This dictates that rGO is the main acting component for adsorption of heavy metals and NaCl due to its unique physicochemical properties such as large surface area, π-π interaction, porosity, chemical and mechanical strength. Moreover, 10% rGO/NiMoV LDH has shown exceptional salt rejection rate, water flux and reverse solute flux. This indicates that rGO/NiMoV LDH is a favourable candidate for desalination and adsorption of heavy metals. This research possesses huge potential for application in desalination on commercial scale.

6. REFERENCES

1. Dhakal, N. *et al.* Is Desalination a Solution to Freshwater Scarcity in Developing Countries? *Membranes 2022, Vol. 12, Page 381* **12**, 381 (2022).
2. Dhakal, N., Salinas Rodriguez, S. G., Schippers, J. C. & Kennedy, M. D. Perspectives and challenges for desalination in developing countries. *IDA Journal of Desalination and Water Reuse* **6**, 10–14 (2014).
3. Esmaeilion, F. *et al.* Renewable energy desalination; a sustainable approach for water scarcity in al dirands. *https://doi.org/10.1080/19397038.2021.1948143* **14**, 1916–1942 (2021).
4. Geise, G. M. *et al.* Water purification by membranes: The role of polymer science. *J Polym Sci B Polym Phys* **48**, 1685–1718 (2010).
5. Xu, J., Li, P., Jiao, M., Shan, B. & Gao, C. Effect of Molecular Configuration of Additives on the Membrane Structure and Water Transport Performance for Forward Osmosis. *ACS Sustain Chem Eng* **4**, 4433–4441 (2016).
6. Yip, N. Y., Tiraferri, A., Phillip, W. A., Schiffman, J. D. & Elimelech, M. High performance thin-film composite forward osmosis membrane. *Environ Sci Technol* **44**, 3812–3818 (2010).
7. Suwaileh, W., Pathak, N., Shon, H. & Hilal, N. Forward osmosis membranes and processes: A comprehensive review of research trends and future outlook. *Desalination* **485**, 114455 (2020).
8. Wang, K. Y., Ong, R. C. & Chung, T. S. Double-skinned forward osmosis membranes for reducing internal concentration polarization within the porous sublayer. *Ind Eng Chem Res* **49**, 4824–4831 (2010).
9. Ray, S. S. *et al.* Developments in forward osmosis and membrane distillation for desalination of waters. *Environ Chem Lett* **16**, 1247–1265 (2018).
10. Yang, Q., Wang, K. Y. & Chung, T. S. Dual-layer hollow fibers with enhanced flux as novel forward osmosis membranes for water production. *Environ Sci Technol* **43**, 2800–2805 (2009).
11. Kahrizi, M. *et al.* Significant roles of substrate properties in forward osmosis membrane performance: A review. *Desalination* **528**, 115615 (2022).

12. He, M. *et al.* Stable Forward Osmosis Nanocomposite Membrane Doped with Sulfonated Graphene Oxide@Metal-Organic Frameworks for Heavy Metal Removal. *ACS Appl Mater Interfaces* **12**, 57102–57116 (2020).
13. Wang, K. Y., Chung, T. S. & Amy, G. Developing thin-film-composite forward osmosis membranes on the PES/SPSf substrate through interfacial polymerization. *AIChE Journal* **58**, 770–781 (2012).
14. Yadav, S. *et al.* Recent developments in forward osmosis membranes using carbon-based nanomaterials. *Desalination* vol. 482 Preprint at https://doi.org/10.1016/j.desal.2020.114375 (2020).
15. Wang, L. *et al.* Salt and Water Transport in Reverse Osmosis Membranes: Beyond the Solution-Diffusion Model. *Environ Sci Technol* **55**, 16665–16675 (2021).
16. Esmaeilion, F. Hybrid renewable energy systems for desalination. *Appl Water Sci* **10**, (2020).
17. Mehdinia, A., Heydari, S. & Jabbari, A. Synthesis and characterization of reduced graphene oxide-Fe3O4@polydopamine and application for adsorption of lead ions: Isotherm and kinetic studies. *Mater Chem Phys* **239**, (2020).
18. Cui, Y., Ge, Q., Liu, X. Y. & Chung, T. S. Novel forward osmosis process to effectively remove heavy metal ions. *J Memb Sci* **467**, 188–194 (2014).
19. Zhang, B. L. *et al.* Mechanism study about the adsorption of Pb(II) and Cd(II) with iron-trimesic metal-organic frameworks. *Chemical Engineering Journal* **385**, 123507 (2020).
20. Tee, G. T., Gok, X. Y. & Yong, W. F. Adsorption of pollutants in wastewater via biosorbents, nanoparticles and magnetic biosorbents: A review. *Environmental Research* vol. 212 Preprint at https://doi.org/10.1016/j.envres.2022.113248 (2022).
21. Gherbi, B. *et al.* Effect of pH Value on the Bandgap Energy and Particles Size for Biosynthesis of ZnO Nanoparticles: Efficiency for Photocatalytic Adsorption of Methyl Orange. *Sustainability (Switzerland)* **14**, (2022).
22. He, M. *et al.* Novel polydopamine/metal organic framework thin film nanocomposite forward osmosis membrane for salt rejection and heavy metal removal. *Chemical Engineering Journal* **389**, 124452 (2020).
23. Kalam, S., Abu-Khamsin, S. A., Kamal, M. S. & Patil, S. Surfactant Adsorption Isotherms: A Review. *ACS Omega* **6**, 32342–32348 (2021).

24. Saeedi-Jurkuyeh, A., Jafari, A. J., Kalantary, R. R. & Esrafili, A. A novel synthetic thin-film nanocomposite forward osmosis membrane modified by graphene oxide and polyethylene glycol for heavy metals removal from aqueous solutions. *React Funct Polym* **146**, 104397 (2020).
25. Deka, P. *et al.* Performance evaluation of reduced graphene oxide membrane doped with polystyrene sulfonic acid for forward osmosis process. *Sustainable Energy Technologies and Assessments* **44**, 101093 (2021).
26. Romaniak, G. *et al.* Impact of a graphene oxide reducing agent on a semi-permeable graphene/reduced graphene oxide forward osmosis membrane filtration efficiency. *Membranes (Basel)* **11**, (2021).
27. Lin, G. *et al.* Co3O4 /N-doped RGO nanocomposites derived from MOFs and their highly enhanced gas sensing performance. *Sens Actuators B Chem* **303**, (2020).
28. Lin, Z., Weng, X., Ma, L., Sarkar, B. & Chen, Z. Mechanistic insights into Pb(II) removal from aqueous solution by green reduced graphene oxide. *J Colloid Interface Sci* **550**, 1–9 (2019).
29. Wu, W., Shi, Y., Liu, G., Fan, X. & Yu, Y. Recent development of graphene oxide based forward osmosis membrane for water treatment: A critical review. *Desalination* vol. 491 Preprint at https://doi.org/10.1016/j.desal.2020.114452 (2020).
30. Fan, X., Liu, Y. & Quan, X. A novel reduced graphene oxide/carbon nanotube hollow fiber membrane with high forward osmosis performance. *Desalination* 117–124 (2019) doi:10.1016/j.desal.2018.07.020.
31. Mutharasi, Y., Zhang, Y., Weber, M., Maletzko, C. & Chung, T. S. Novel reverse osmosis membranes incorporated with Co-Al layered double hydroxide (LDH) with enhanced performance for brackish water desalination. *Desalination* **498**, (2021).
32. Bagherzadeh, M., Nikkhoo, M., Ahadian, M. M. & Amini, M. Novel Thin-Film Nanocomposite Forward Osmosis Membranes Modified with WS2/CuAl LDH Nanocomposite to Enhance Desalination and Anti-fouling Performance. *J Inorg Organomet Polym Mater* **33**, 956–968 (2023).
33. Lei, J., Xiong, Y., Yu, F. & Ma, J. Flexible self-supporting CoFe-LDH/MXene film as a chloride ions storage electrode in capacitive deionization. *Chemical Engineering Journal* **437**, (2022).

34. Wang, Z. *et al.* Modulating electronic structure of ternary NiMoV LDH nanosheet array induced by doping engineering to promote urea oxidation reaction. *Chemical Engineering Journal* **430**, (2022).
35. Li, Z. *et al.* rGO/protonated g-C3N4 hybrid membranes fabricated by photocatalytic reduction for the enhanced water desalination. *Desalination* **443**, 130–136 (2018).
36. Bodzek, M. & Konieczny, K. Nanomaterials in membrane water desalination. *Desalination Water Treat* **214**, 155–180 (2021).
37. Asif, M. B., Kang, H. & Zhang, Z. Gravity-driven layered double hydroxide nanosheet membrane activated peroxymonosulfate system for micropollutant degradation. *J Hazard Mater* **425**, (2022).
38. Kotp, Y. H. High-flux TFN nanofiltration membranes incorporated with Camphor-Al2O3 nanoparticles for brackish water desalination. *Chemosphere* **265**, (2021).
39. Moshari, M., Mehrehjedy, A., Heidari-Golafzania, M., Rabbani, M. & Farhadi, S. Adsorption study of lead ions onto sulfur/reduced graphene oxide composite. *Chemical Data Collections* **31**, (2021).
40. Dong, Y. *et al.* Single-layered GO/LDH hybrid nanoporous membranes with improved stability for salt and organic molecules rejection. *J Memb Sci* **607**, (2020).
41. Kahrizi, M. *et al.* Significant roles of substrate properties in forward osmosis membrane performance: A review. *Desalination* vol. 528 Preprint at https://doi.org/10.1016/j.desal.2022.115615 (2022).
42. Pouya, Z. A., Tofighy, M. A. & Mohammadi, T. Synthesis and characterization of polytetrafluoroethylene/oleic acid-functionalized carbon nanotubes composite membrane for desalination by vacuum membrane distillation. *Desalination* **503**, (2021).
43. de Biasi, L. *et al.* Phase Transformation Behavior and Stability of LiNiO2 Cathode Material for Li-Ion Batteries Obtained from In Situ Gas Analysis and Operando X-Ray Diffraction. *ChemSusChem* **12**, 2240–2250 (2019).
44. Guerrero-Pérez, M. O. & Patience, G. S. Experimental methods in chemical engineering: Fourier transform infrared spectroscopy—FTIR. *Canadian Journal of Chemical Engineering* vol. 98 25–33 Preprint at https://doi.org/10.1002/cjce.23664 (2020).

45. Chen, Y. *et al.* Acid-salt treated CoAl layered double hydroxide nanosheets with enhanced adsorption capacity of methyl orange dye. *J Colloid Interface Sci* **548**, 100–109 (2019).
46. Yang, L. *et al.* Fabrication of poly(o-phenylenediamine)/reduced graphene oxide composite nanosheets via microwave heating and their effective adsorption of lead ions. *Appl Surf Sci* **307**, 601–607 (2014).
47. Huang, H. H., Joshi, R. K., De Silva, K. K. H., Badam, R. & Yoshimura, M. Fabrication of reduced graphene oxide membranes for water desalination. *J Memb Sci* **572**, 12–19 (2019).